AD-A171 170 MILITARY HYDROLOGY REPORT 10 ASSESSMENT AND FIELD EXAMPLES OF CONTINUOUS (U) ARMY ENGINEER WATERWAYS EXPERIMENT STATION VICKSBURG MS ENVIR D K BUTLER

1/1

UNCLASSIFIED JUN 86 WES/MP/EL/79-6 F/G 8/8 NL

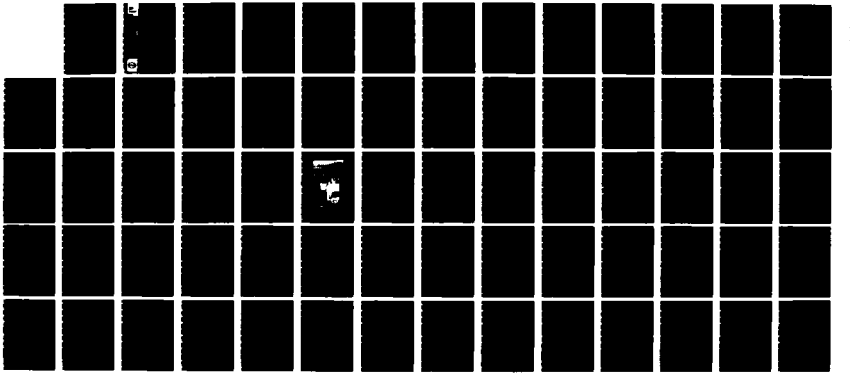

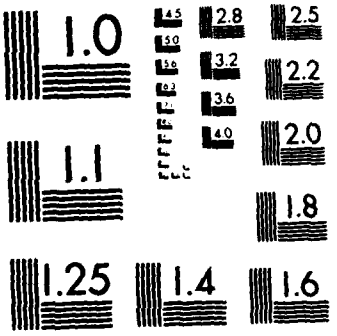

US Army Corps of Engineers

AD-A171 170

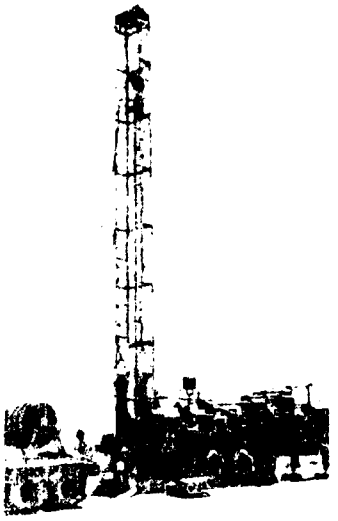

ENVIRONMENTAL LABORATORY

DTIC FILE COPY

MISCELLANEOUS PAPER EL-79-6

MILITARY HYDROLOGY

Report 10

ASSESSMENT AND FIELD EXAMPLES OF CONTINUOUS WAVE ELECTROMAGNETIC SURVEYING FOR GROUND WATER

by

Dwain K. Butler

Geotechnical Laboratory

DEPARTMENT OF THE ARMY
Waterways Experiment Station, Corps of Engineers
PO Box 631, Vicksburg, Mississippi 39180-0631

June 1986

Report 10 of a Series

Prepared for DEPARTMENT OF THE ARMY
US Army Corps of Engineers
Washington, DC 20314-1000

Under DA Project No. 4A762719AT40
Task Area CO, Work Unit 017

and US Army Belvoir Research, Development, and Engineering Center
Fort Belvoir, Virginia 22060-5605

Under Project Order No. A3297

Monitored by Environmental Laboratory
US Army Engineer Waterways Experiment Station
PO Box 631, Vicksburg, Mississippi 39180-0631

MILITARY HYDROLOGY REPORTS

Report No.	No. in Series	Title	Date
TR EL-79-2	-	Proceedings of the Military Hydrology Workshop, 17-19 May 1978, Vicksburg, Mississippi	May 1979
MP EL-79-6 (Military Hydrology Series)	1	Status and Research Requirements	Dec 1979
	2	Formulation of a Long-Range Concept for Streamflow Prediction Capability	Jul 1980
	3	A Review of Army Doctrine on Military Hydrology	Jun 1981
	4	Evaluation of an Automated Water Data Base for Support to the Rapid Deployment Joint Task Force (RDJTF)	Nov 1981
	5	A Quantitative Summary of Groundwater Yield, Depth, and Quality Data for Selected Mideast Areas (U)	Mar 1982
	6	Assessment of Two Currently "Fieldable" Geophysical Methods for Military Ground-Water Detection	Oct 1984
	7	A Statistical Summary of Ground-Water Yield, Depth, and Quality Data for Selected Areas in the CENTCOM Theatre of Operations (U)	Oct 1984
	8	Feasibility of Using Satellite and Radar Data in Hydrologic Forecasting	Sep 1985
	9	State-of-the-Art Review and Annotated Bibliography of Dam-Breach Flood Forecasting	Feb 1985
	10	Assessment and Field Examples of Continuous Wave Electromagnetic Surveying for Ground Water	Jun 1986

Unclassified

SECURITY CLASSIFICATION OF THIS PAGE *(When Data Entered)*

REPORT DOCUMENTATION PAGE

READ INSTRUCTIONS BEFORE COMPLETING FORM

1. REPORT NUMBER: Miscellaneous Paper EL-79-6
2. GOVT ACCESSION NO.: ADA 171170
3. RECIPIENT'S CATALOG NUMBER:

4. TITLE *(and Subtitle)*: MILITARY HYDROLOGY; Report 10: ASSESSMENT AND FIELD EXAMPLES OF CONTINUOUS WAVE ELECTROMAGNETIC SURVEYING FOR GROUND WATER

5. TYPE OF REPORT & PERIOD COVERED: Report 10 of a series

6. PERFORMING ORG. REPORT NUMBER:

7. AUTHOR(s): Dwain K. Butler

8. CONTRACT OR GRANT NUMBER(s):

9. PERFORMING ORGANIZATION NAME AND ADDRESS: US Army Engineer Waterways Experiment Station, Geotechnical Laboratory, PO Box 631, Vicksburg, Mississippi 39180-0631

10. PROGRAM ELEMENT, PROJECT, TASK AREA & WORK UNIT NUMBERS: DA Project No. 4A762719AT40, Task Area CO, Work Unit 017; Project Order No. A3297

11. CONTROLLING OFFICE NAME AND ADDRESS: DEPARTMENT OF THE ARMY, US Army Corps of Engineers, Washington, DC 20314-1000; US Army Belvoir Research, Development, and Engineering Center, Fort Belvoir, Virginia 22060-5605

12. REPORT DATE: June 1986

13. NUMBER OF PAGES: 63

14. MONITORING AGENCY NAME & ADDRESS *(if different from Controlling Office)*: US Army Engineer Waterways Experiment Station, Environmental Laboratory, PO Box 631, Vicksburg, Mississippi 39180-0631

15. SECURITY CLASS. *(of this report)*: Unclassified

15a. DECLASSIFICATION/DOWNGRADING SCHEDULE:

16. DISTRIBUTION STATEMENT *(of this Report)*

Approved for public release; distribution unlimited.

17. DISTRIBUTION STATEMENT *(of the abstract entered in Block 20, if different from Report)*

18. SUPPLEMENTARY NOTES

Available from National Technical Information Service, 5285 Port Royal Road, Springfield, Virginia 22161.

19. KEY WORDS *(Continue on reverse side if necessary and identify by block number)*

Electromagnetic methods
Geophysics
Ground water
Military hydrology

20. ABSTRACT *(Continue on reverse side if necessary and identify by block number)*

This report reviews the concept of a particular type of electromagnetic (EM) geophysical method applied to ground-water exploration and assessment. The method utilizes a transmitter with a small loop antenna, which is excited with a continuous wave (CW) EM signal. The magnetic field generated by the transmitter couples inductively with subsurface geological materials and generates eddy currents. The secondary magnetic fields generated by the eddy

(Continued)

DD FORM 1 JAN 73 1473 EDITION OF 1 NOV 65 IS OBSOLETE

Unclassified

SECURITY CLASSIFICATION OF THIS PAGE *(When Data Entered)*

20. ABSTRACT (Continued).

currents couple inductively with a receiver with a small loop antenna. The specific system type considered in this report operates under the conditions which allow a "small induction number approximation" to be made. This approximation allows the receiver response to be calibrated directly in terms of apparent ground conductivity. By operating the system at multiple transmitter and receiver coil spacings and multiple transmitter frequencies, it is possible to conduct EM soundings.

A specific CW EM system was field tested at White Sands, N. Mex., and Fort Carson, Colo., at locations where previous geophysical surveys were conducted using seismic and electrical resistivity methods. For the White Sands EM surveys, a critical evaluation of data interpretation procedures is presented. Specifically, the EM interpretations are compared to models deduced from the previous geophysical work at the locations. At Fort Carson, an EM sounding was conducted at 20-m intervals along a 700-m profile line. Also, an EM sounding was conducted on an outcrop of Dakota Sandstone.

The results of an EM sounding can be interpreted, in principle, to yield a model of the vertical variation in electrical conductivity in the subsurface. In some cases the conductivity model can be interpreted in terms of a hydrogeological model, although supplementary geological data or complementary geophysical data are usually required. Analysis of the White Sands EM survey results indicates the multilayer response calculations, for predicting the low induction number performance of the device, should be used with caution because the response functions overpredict the proportion of the response from deeper layers. For three of the five cases, two-layer equivalent model interpretations of the EM data are useful and correlate satisfactorily with resistivity models. The most useful interpretation procedure is to assign measured apparent conductivities to rule-of-thumb depths of investigation and use the model only as a qualitative indicator of the conductivity versus depth variation. At Fort Carson, the conductivities measured on the outcrop agreed with values deduced for the sandstone in the subsurface from a resistivity sounding. The EM data along the Fort Carson profile line agreed well with a geological model for the site deduced from available geological information, site reconnaissance, and previous geophysical surveys.

The EM device evaluated in this study is lightweight and easy to operate in the field; surveys proceed rapidly. These comments apply in general to CW EM systems. The device considered in this report could not "stand alone" nor replace electric resistivity in a complementary methods approach for groundwater detection and assessment. However, the device can be useful as a rapid survey technique to supplement resistivity surveys in a complementary methods approach. The CW EM methods are not limited to the small number of conductivity determinations (coil spacing-frequency combinations) of the device considered here. Currently available CW EM systems with greater capability and applicability, however, are larger and more cumbersome to use, and the data interpretation is not as straightforward.

PREFACE

This work was performed during the period August 1983 to August 1984 by personnel of the Earthquake Engineering and Geophysics Division (EEGD), Geotechnical Laboratory (GL), US Army Engineer Waterways Experiment Station (WES). The effort was funded by the Office, Chief of Engineers (OCE), US Army, under Department of the Army Project No. 4A762719AT40, "Mobility, Soils, and Weapons Effects Technology," Task Area CO, Work Unit 017, "Remote Procedures for Locating Water Supplies," and by the US Army Belvoir Research, Development, and Engineering Center (BRDEC), Fort Belvoir, Va., under Project Order No. A3297, dated 2 August 1983. Dr. Clemens A. Meyer was the OCE Technical Monitor. CPT Robert Thompson was the point of contact for BRDEC.

Mr. José L. Llopis, 1LT Stephen G. Sanders, and Dr. Dwain K. Butler conducted the work under the general supervision of Dr. Arley G. Franklin, Chief, EEGD, and Dr. William F. Marcuson III, Chief, GL. This report was prepared by Dr. Butler.

Principal Investigators of Work Unit 017 are Messrs. Elba A. Dardeau, Jr., and John G. Collins, Environmental Constraints Group (ECG), Environmental Systems Division (ESD), Environmental Laboratory (EL). The work unit is under the general supervision of Mr. Malcolm P. Keown, Chief, ECG; Dr. Lewis E. Link, Chief, ESD; and Dr. John Harrison, Chief, EL. This report was edited by Ms. Jessica S. Ruff of the WES Publications and Graphic Arts Division.

Director of WES was COL Allen F. Grum, USA. Technical Director was Dr. Robert W. Whalin.

This report should be cited as follows:

Butler, D. K. 1986. "Military Hydrology; Report 10: Assessment and Field Examples of Continuous Wave Electromagnetic Surveying for Ground Water," Miscellaneous Paper EL-79-6, US Army Engineer Waterways Experiment Station, Vicksburg, Miss.

A-1

CONTENTS

MILITARY HYDROLOGY

ASSESSMENT AND FIELD EXAMPLES OF CONTINUOUS WAVE ELECTROMAGNETIC SURVEYING FOR GROUND WATER

PART I: INTRODUCTION

Background

1. Military hydrology is a specialized field of study that deals with the effects of surface and subsurface water on the planning and conduct of military operations. In 1977, the Office, Chief of Engineers, approved a military hydrology research program; management responsibility was subsequently assigned to the Environmental Laboratory, US Army Engineer Waterways Experiment Station (WES), Vicksburg, Miss.

2. The objective of military hydrology research is to develop an improved hydrologic capability for the Armed Forces with emphasis on application in the tactical environment. To meet this overall objective, research is being conducted in four thrust areas: (a) weather-hydrology interactions; (b) state of the ground; (c) streamflow; and (d) water supply.

3. Previously published Military Hydrology reports are listed on the inside of the front cover. This report is the fifth that contributes to the water-supply thrust area, which is oriented toward the development of an integrated methodology for rapidly locating and evaluating ground-water supplies, particularly in arid regions. Specific work efforts include: (a) the compilation of guidelines for the expedient location of water for human survival, (b) the development of remote imagery interpretation procedures for detecting and evaluating ground-water sources, (c) the adaptation of suitable geophysical methods for detecting and evaluating ground-water sources, and (d) the development of water-supply analysis and display concepts.

4. Water supply, particularly in arid regions, has been identified as a high-priority problem for the military. Surface water supplies are inadequate, unreliable, and unpredictable in many arid regions of strategic importance; thus, the capability of detecting producible ground-water resources in such areas is critically important. However, technology shortfalls exist in surface techniques for detection of ground water.

5. A Ground-Water Detection Workshop was held in Vicksburg, Miss., in January 1982 to consider, among other topics, the technology shortfalls in surface techniques for detection of ground water. The conclusions of the Geophysics Working Group at the Workshop were: (a) two currently fieldable geophysical methods (electrical resistivity and seismic refraction) are applicable to the ground-water detection problem and may offer a near-term solution to the technology shortfall, and (b) several state-of-the-art and emerging geophysical techniques may have potential for the long-term solution.

6. In May 1982, the US Army Mobility Research and Development Command (now US Army Belvoir Research, Development, and Engineering Center) funded a study to assess the complementary application of electrical resistivity and seismic refraction geophysical methods as a near-term solution to the technology shortfall in surface ground-water detection capability. Report 6 of this series (Butler and Llopis 1984) presents the results of that study. Two sites were selected for field demonstration and evaluation of the complementary geophysical survey approach to ground-water detection. At White Sands Missile Range, N. Mex., five locations were tested with water table depths in alluvial materials ranging from 20 to 137 m. A confined rock aquifer at a depth of about 82 m was the detection objective at the Fort Carson, Colo., site.

7. Results of geophysical surveys at the White Sands site included four cases of successful ground-water table detection, with errors in predicted depth ranging from 12 to 28 percent, and one case in which the table was erroneously interpreted. At the Fort Carson site, topographic variations and lateral material variations prevented a definitive ground-water detection assessment. Also, as will be discussed later in this report, there were uncertainties in the hydrogeological model for comparison with the geophysical data.

8. Results of the above geophysical field studies and other similar studies show that:

   a. For cases where the water table occurs in coarse-grained sediments (sands and gravels), the geophysical methods can be used very successfully for ground-water detection.

   b. For cases where the water table occurs in fine-grained sediments (clayey sands, silts, silty clays, sandy clays, etc.), the geophysical methods can be used for ground-water detection; however, the interpretation will sometimes not be as straightforward as for case a, and the difference between predicted and

actual water table depth can sometimes be much greater than for case a.

c. A freshwater/saltwater interface is easily detected by the resistivity method but will not show as an interface in seismic refraction results; detection of this interface is useful in that any freshwater present will be shallower than the interface depth.

d. Rock aquifers can be detected by the geophysical methods, but there may be nothing in the survey results to differentiate a rock aquifer from an unsaturated rock unit (except for the case where the rock unit has high resistivity, in which case the unit is not an aquifer).

e. For some field situations, such as at the Fort Carson site, topographic variations and complex, lateral geologic changes make a straightforward data interpretation impossible.

f. In some cases, such as the HTA-1 location at White Sands, the straightforward interpretation method will lead to false identification of the water table.

The above conclusions show that complementary seismic refraction and electrical resistivity surveys can (a) generally be used successfully for ground-water detection when the water table occurs in unconsolidated sediments and (b) generally not be used successfully for detection of ground water in confined rock aquifers. For the case of rock aquifers, a ground-water exploration program is required.

9. The distinction between detection and exploration applications of geophysical methods is thoroughly discussed in Report 6 of this series. Briefly, a geophysical ground-water exploration program will use all available borehole and other geological data in order to produce the best possible assessment of the ground-water potential and conditions in an area. The primary objective of geophysical ground-water exploration is the mapping of subsurface structural and stratigraphic indicators of the possible occurrence of the ground water, such as buried river channels, fracture zones in bedrock, confining layers (aquacludes), etc. Actual detection of the ground-water table with any of the geophysical surveys may be noted but may not be of primary importance in the overall ground-water exploration assessment.

10. The expression "ground-water detection," as used in this report, in contrast to ground-water exploration, applies to the concept of detecting the presence (or absence) of ground water and the depth to the water table beneath a given "point" on the surface by conducting one or more types of geophysical tests at that point. In the ideal case, the aquifer thickness and water

quality would also be determined. For some cases, information regarding ground-water occurrence and other geological factors might be available but, in general, the assessment of the presence of ground water must rely solely on the geophysical results at the given surface location in the detection scenario. In many cases, geophysical ground-water surveys will probably be required to select a site from among these alternate sites already identified by other methods as having good ground-water potential.

11. Investigation of state-of-the-art and emerging geophysical methodologies indicates several electromagnetic (EM) techniques in geophysics which may be applicable to the ground-water detection problem. Generally, the EM survey data are interpreted to provide essentially the same geophysical model as the electrical resistivity method; however, the EM surveys are usually simpler to conduct and offer other advantages which will be examined in this report.

12. Although a considerable oversimplification, EM methods in geophysics can be classified as either wave propagation or induction methods, denoting the dominant physical mechanisms exploited. The so-called ground-penetrating radars, used for various geotechnical applications, are an example of devices exploiting EM wave propagation. In turn, two primary classes of EM induction methods, transient and continuous wave (CW) systems, are in use for various applications ranging from deep crustal sounding to mineral exploration.

Objectives

13. Objectives of this investigation are: (a) to assess the applicability of CW EM induction methods to the ground-water detection problem and (b) to field test a commercially available CW EM system at sites for which geophysical and hydrogeological information is available.

Scope

14. The investigation reported herein includes the following considerations:

a. A brief review of the concepts of EM induction methods.

b. A brief survey of pertinent reported applications of EM methods to ground-water exploration and detection.

c. A discussion of the theory of operation, field procedures, and interpretation methods for the CW EM system selected for the field studies.

d. Presentation and analysis of the results of field studies at White Sands, N. Mex., and Fort Carson, Colo.

e. Conclusions and recommendations regarding the applicability of CW EM methods in complementary geophysical surveys for ground-water detection.

PART II: ELECTROMAGNETIC SURVEYING CONCEPTS

Definitions

15. The behavior of electromagnetic fields within a region with electrical conductivity σ, dielectric constant ϵ, and magnetic permeability μ is governed by Maxwell's equations, which are four differential relations between the following five field vectors:

$\bar{B}$ - magnetic induction in webers per square metre

$\bar{H}$ - magnetic field intensity in ampere-turns per metre

$\bar{D}$ - electric displacement in coulombs per square metre

$\bar{E}$ - electric field intensity in volts per metre

$\bar{J}$ - electric current density in amperes per square metre

Using three constitutive relations between the field vectors, $\bar{B} = \mu\bar{H}$, $\bar{D} = \epsilon\bar{E}$, and $\bar{J} = \sigma\bar{E}$, which hold for most isotropic materials, the following differential equations for the electric and magnetic field intensities can be derived from Maxwell's equations:

$$\nabla^2\bar{E} - \sigma\mu \frac{\partial\bar{E}}{\partial t} - \epsilon\mu \frac{\partial^2\bar{E}}{\partial t^2} = 0 \tag{1}$$

and

$$\nabla^2\bar{H} - \sigma\mu \frac{\partial\bar{H}}{\partial t} - \epsilon\mu \frac{\partial^2\bar{H}}{\partial t^2} = 0 \tag{2}$$

16. For all the considerations in this report, CW or harmonic time variations are considered; for example, $\bar{E}(t) = \bar{E}_o e^{i\omega t}$, where $\bar{E}_o$ is the amplitude, $i = \sqrt{-1}$, and ω is the radian frequency of the electric field intensity. Equations 1 and 2 thus simplify to

$$\nabla^2\bar{E} - i\sigma\mu\omega\bar{E} + \epsilon\mu\omega^2\bar{E} = 0 \tag{3a}$$

or

$$\nabla^2\bar{H} - \gamma^2\bar{E} = 0 \tag{3b}$$

and

$$\nabla^2\bar{H} - i\sigma\mu\omega\bar{H} + \epsilon\mu\omega^2\bar{H} = 0 \tag{4a}$$

or

$$\nabla^2\bar{H} - \gamma^2\bar{H} = 0 \tag{4b}$$

where

$$\begin{aligned}\gamma^2 &= i\omega\mu\sigma - \varepsilon\mu\omega^2 \\ &= i\omega\mu(\sigma + i\omega\varepsilon)\end{aligned} \tag{5}$$

The parameter γ is called the propagation factor. Solutions to Equation 3 will be of the form $e^{-\gamma z}$ for propagation in the z-direction. If the propagation factor is expressed in the form $\gamma = \alpha + i\beta$, the factor $e^{-\alpha z}$ represents a damping, attenuation, or dissipation factor, while $e^{-i\beta z}$ represents wave propagation. Thus, for the general case, solutions to Equations 3 and 4 will represent dissipative wave motion.

17. In addition to α, two other parameters are commonly used to describe dissipation or energy loss during EM wave motion in a medium; these are the skin depth δ, which is related to α by $\delta = 1/\alpha$, and the loss tangent $\tan\theta$. Physically, the skin depth is the propagation distance in a medium required to attenuate an electromagnetic component to $1/e$ of its initial value, and the loss tangent is the ratio of conduction currents to displacement currents in the medium. In terms of previously defined parameters,

$$\tan\theta = \frac{\sigma}{\omega\varepsilon} \tag{6}$$

$$\alpha = \omega\sqrt{\frac{\mu\varepsilon}{2}}\left[\left(1 + \tan^2\theta\right)^{1/2} - 1\right]^{1/2} \tag{7}$$

and

$$\delta = \frac{1}{\alpha} \tag{8}$$

Thus, the parameters α, δ, and $\tan\theta$ are related to each other and are functions of frequency and the conductivity of the medium.

Depth Sounding Methods

18. The electromagnetic methods considered in this report involve the use of loop transmitters at the ground surface. A current $I = I_o e^{i\omega t}$ in the transmitter coil produces a magnetic field that closely approximates the field of a magnetic dipole with moment $m = IA$, where A is the loop area, for observation points (the receiver) that are several loop diameters from the transmitter. The frequencies of interest are low enough and the transmitter-receiver separations small enough (considerably less than a free space wave length) that all coupling between transmitter and receiver, transmitter and earth, and earth and receiver is inductive in nature, as illustrated in Figure 1 for an idealized, isolated conductive body in the subsurface. The time-varying primary magnetic field $\bar{H}_p$ of the transmitter penetrates the earth, to a depth which depends on the signal frequency and the conductivity and other EM parameters of the subsurface, and generates eddy currents in the subsurface materials (as illustrated in Figure 1). The eddy currents, in turn, generate secondary magnetic fields that form a secondary field $\bar{H}_s$ which interacts with the receiver along with $\bar{H}_p$.

19. Vertical or depth sounding refers to a procedure for investigating the variation of EM properties as a function of depth within the earth. The depth of investigation is limited to the maximum depth at which a secondary magnetic field can be generated with sufficient magnitude at the receiver to produce a detectable response of the EM induction system described above. The depth of investigation depends on the frequency, EM parameters of the subsurface, subsurface geometry, and distance between transmitter (Tx) and receiver (Rx).

20. In principle, a vertical or depth sounding at a given location could be accomplished in two ways: (a) by varying the frequency, known as parametric sounding, or (b) by varying the Tx-Rx separation, known as geometric sounding. Examination of Equations 6-8 reveals the principle of parametric sounding--as the frequency decreases, the skin depth and, hence, the depth of investigation increase, and vice versa. In principle, parametric sounding is the preferable procedure, since it would require no changes in Tx-Rx locations and thus would not be significantly affected by lateral variations. However, for a given frequency, there is generally an optimum Tx-Rx separation

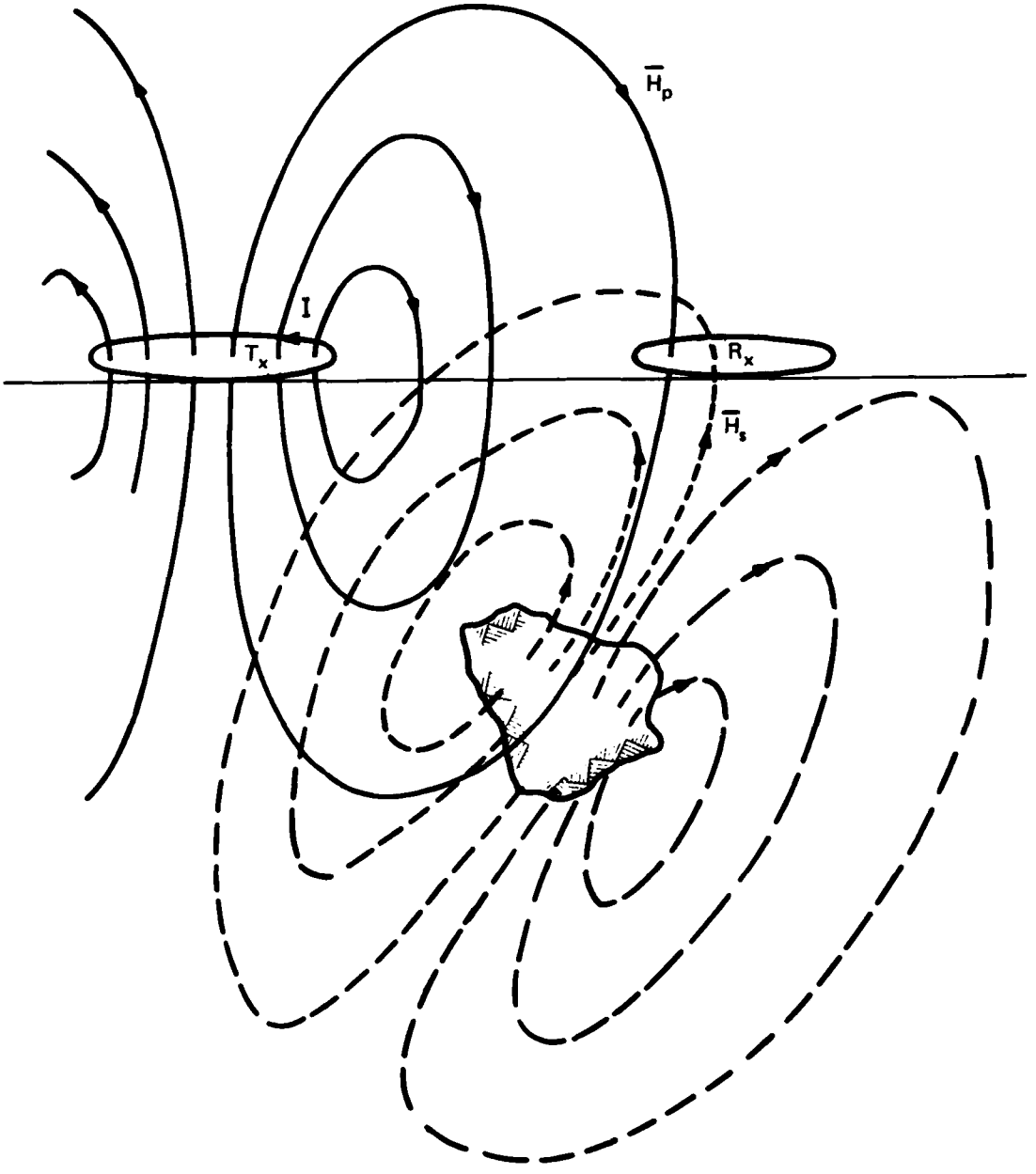

Figure 1. Illustration of inductive coupling between transmitter (Tx), receiver (Rx), and conductive body; $\bar{H}_p$ and $\bar{H}_s$ are the primary and secondary magnetic fields, respectively

that gives maximum response sensitivity to EM properties at a given depth. Thus, in practice, it is common to vary both frequency and Tx-Rx separations during a sounding. Also, the maximum practical depth of investigation for a given intercoil spacing will be between one and five times the Tx-Rx spacing regardless of transmitter power.

Horizontal Profiling

21. For a fixed transmitter frequency and Tx-Rx spacing, the depth of investigation will depend only on the EM and geometric properties of the subsurface. If the transmitter and receiver are translated along a profile line keeping frequency and spacing constant, variations in the secondary field will reflect variations in EM properties (such as lateral variations in soil or rock type) and/or subsurface geometry (such as variations in depths to interfaces) within the depth of investigation, although strictly speaking, the depth of investigation itself will vary as the other parameters vary. This type of EM survey, with constant transmitter frequency and Tx-Rx spacing, is called horizontal profiling.

The Long-Wavelength Approximation and Quasi-Static Considerations

22. For distances that are small compared to the free space wavelength of the transmitter signal, the EM fields are quasi-static in the sense that, while the $e^{i\omega t}$ time variation holds for all the fields, the fields are essentially in phase with the transmitter current. This quasi-static condition can be likened to instantaneous field propagation, and phase retardation and wave propagation effects can be neglected. The second term in Equations 3a and 4a is related to conduction currents while the last term is related to displacement currents; examination of the relative magnitudes of the coefficients of these terms reveals that, for all practical cases of interest, the displacement current term can be neglected when quasi-static conditions hold.

23. Consider, for example, a frequency $f = 10^5$ Hz ($\omega = 2\pi f$), which is higher than used in any typical field CW EM system. For most soil and rock, $\mu \approx \mu_o \approx 1.3 \times 10^{-6}$ H/m and $\varepsilon \approx 9\varepsilon_o \approx 8 \times 10^{-11}$ F/m , where the subscript

denotes the free space values. Most commonly encountered soil and rock types have a conductivity range of 10^{-3} to 10^{2} mho/m; for the extremes of this conductivity range, the coefficients have the following values:

f = 100 kHz	$\sigma = 10^{-3}$ mho/m	$\sigma = 10^{2}$ mho/m
Displacement current term coefficient	4.1×10^{-5}	4.1×10^{-5}
Conduction current term coefficient	8.2×10^{-4}	82

Thus, even for the extreme case of $f = 10^{5}$ Hz and $\sigma = 10^{-3}$ mho/m, the conduction current term is 20 times greater than the displacement current term. In general, therefore, the effects of displacement currents can be neglected for the class of EM problems and survey systems considered in this report, and Equations 3 and 4 reduce to

$$\nabla^2 \begin{Bmatrix} \bar{E} \\ \bar{H} \end{Bmatrix} - i\sigma\mu\omega \begin{Bmatrix} \bar{E} \\ \bar{H} \end{Bmatrix} = 0$$

or

$$\nabla^2 \begin{Bmatrix} \bar{E} \\ \bar{H} \end{Bmatrix} - \sigma\mu \frac{\partial}{\partial t} \begin{Bmatrix} \bar{E} \\ \bar{H} \end{Bmatrix} = 0 \qquad (9)$$

which is a vector diffusion equation. In the region above the ground surface or for essentially nonconducting soil and rock ($\sigma \approx 0$), the relation becomes

$$\nabla^2 \begin{Bmatrix} \bar{E} \\ \bar{H} \end{Bmatrix} \approx 0 \qquad (10)$$

which is the vector Laplace's equation.

24. Since neither Equation 9 nor Equation 10 describes wave propagation, the justification for the term quasi-static becomes more apparent. The conditions under which Equations 9 and 10 describe the EM fields are also variously described as the long-wavelength approximation, the induction zone, and

the near zone or near field (Grant and West 1965, Keller and Frischknecht 1966, Patra and Mallick 1980, Wait 1982, Kaufman and Keller 1983). For various reasons, these terminologies can be misleading; a preferable procedure is to define a dimensionless parameter B, called the induction number, and to state that consideration is limited to the zone where B is small or that a small induction number approximation is made (Kaufman and Keller 1983). The induction number is defined as $B = R/\delta$, where R is the distance from the center of the transmitter loop to the center of the receiver loop or point of observation and δ is the skin depth. Thus, B is a function of the interloop spacing, the transmitter frequency, and the EM parameters of the earth. Neglecting displacement currents, Equation 5 becomes

$$\gamma^2 = i\omega\mu\sigma \tag{11}$$

and

$$\alpha = \beta = \sqrt{\frac{\omega\mu\sigma}{2}}$$

Thus, from Equation 8

$$\sigma = \sqrt{\frac{2}{\omega\mu\sigma}} \tag{12}$$

For any Tx-Rx spacing there will be a frequency below which the small induction number criterion is satisfied, although that frequency also depends on the ground conductivity. Conversely, for any frequency, there is always a zone about the transmitter within which the small induction number criterion is satisfied. Skin depths for selected frequencies and conductivities are as follows.

Skin Depth, m

Conductivity mho/m	Frequency, Hz					
	10	100	500	1,000	5,000	10,000
10^{-3}	4,950	1,565	700	495	220	155
10^{-2}	1,565	495	220	155	70	50
10^{-1}	495	155	70	50	20	15
10^{0}	155	50	20	15	7	5
10^{1}	50	15	7	5	2	1.5
10^{2}	15	5	2	1.5	0.7	0.5

The above tabulation, along with specification of Tx-Rx separation R, allows a quick determination of the value of B for a given case.

25. The zone where B is large generally corresponds to large distances from the transmitter or high frequencies and is variously termed the far field, radiation zone, or wave zone. Again, this latter terminology is misleading, since the displacement currents can generally be neglected except at very high frequencies and/or very low conductivities (e.g., $f > 10^{5}$ Hz and/or $\sigma < 10^{-3}$ mho/m). Equations 9 and 10 describe the fields, and thus the term quasi-static can be applied, even though the free space wavelength may be much less than the distance to the receiver or observation point. Of course, the nature of the fields, i.e., the functional dependence of the fields on frequency, conductivity, and distance, will be different in the small and large induction number zones.

EM Fields for Two-Loop Sounding Arrangements

26. The EM technique specifically considered in this report is based on two-loop arrangements such as shown in Figure 1 and Figures 2a and 2b. Other two-loop arrangements are illustrated in Figures 2c and 2d; in addition, grounded line dipoles can be used for transmitters or receivers. Some systems use magnetometers or ferrite core multiturn coils as receivers. For the cylindrical coordinate system shown in Figure 3, the field components are H_r, H_z, and E_θ. In addition to the magnitude and phase of the field components, receivers can determine the wave tilt H_r/H_z (magnitude and phase), the tilt angle Φ, and the ellipticity H_2/H_1. Of course, determining all of the parameters for a given case requires measurements with different receiver

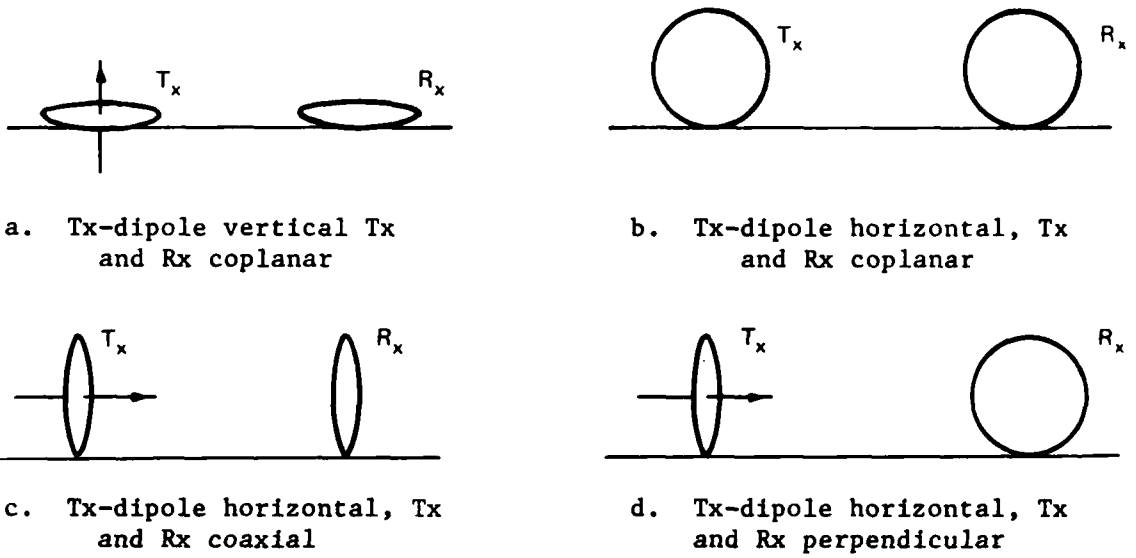

a. Tx-dipole vertical Tx and Rx coplanar

b. Tx-dipole horizontal, Tx and Rx coplanar

c. Tx-dipole horizontal, Tx and Rx coaxial

d. Tx-dipole horizontal, Tx and Rx perpendicular

Figure 2. Examples of two-loop configurations

orientations and/or multiple receivers. For a fixed loop receiver orientation such as that shown in Figure 2a, the H_z component will be determined. For the geometry of Figure 2b, an H_θ component is determined. Actually, the receiver coil measures an induced voltage, which is proportional to the rate of change of magnetic flux through the coil and, hence, to the vector sum of the primary and secondary magnetic fields. While the primary field near the transmitter loop is in phase with the transmitter current, the secondary field is generally not in phase with the transmitter current. Thus, the total field can be considered a complex quantity with real and imaginary (inphase and out-of-phase or quadrature, respectively) components with respect to phase; the terminology inphase and quadrature will be used in this report.

27. On the plane $z = 0$, the primary field components for the vertical magnetic dipole case (Figure 3) are

$$H_{pz} = \frac{m}{4\pi R^3} \tag{13}$$

$$H_{pr} = 0$$

and

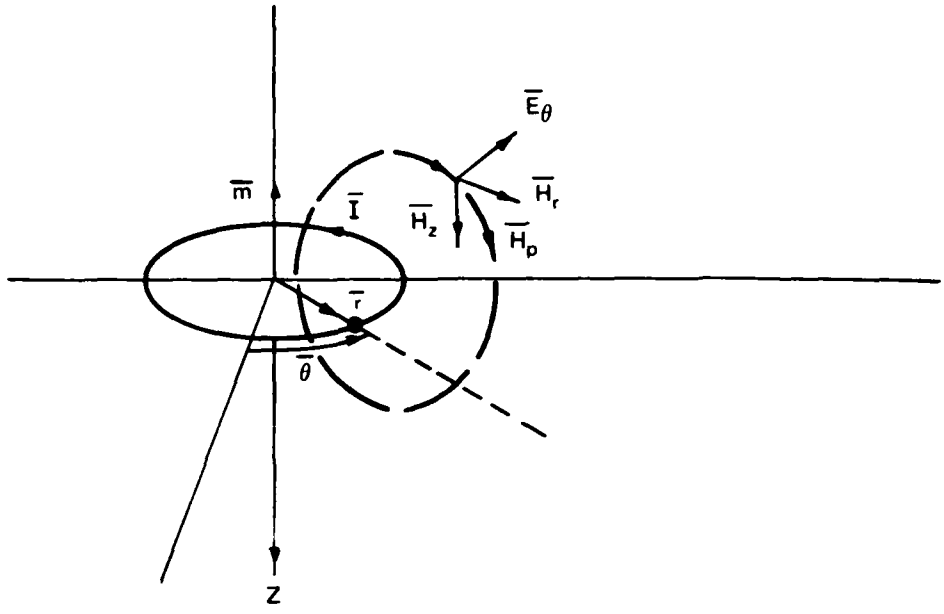

a. Cylindrical coordinate system and primary field components around current-carrying horizontal loop ($\bar{m} = m\hat{n} = IA\hat{n}$, where $\hat{n}$ is unit vector normal to plane of loop)

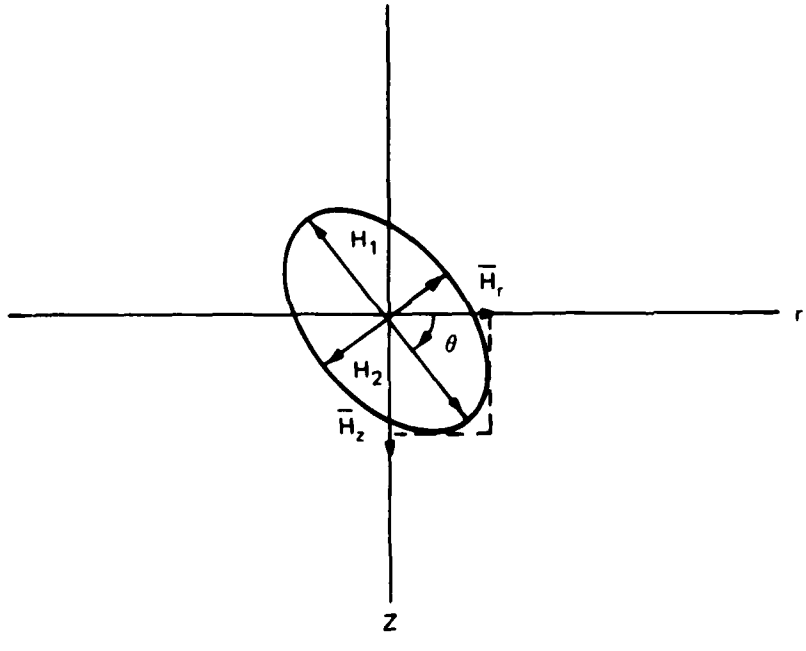

b. Definition of polarization ellipse parameters

Figure 3. Coordinate system and field component definitions

$$E_{p\theta} = \frac{i\omega\mu m}{4\pi R^2}$$

The solution for the total magnetic field intensity H_{tz} on the surface $z = 0$ of a conducting, homogeneous earth is given by (Keller and Frischknecht 1966, Patra and Mallick 1980, Wait 1982, Kaufman and Keller 1983)

$$H_{tz} = H_{pz}\left(\frac{18}{\gamma^2 R^2}\right)\left[1 - e^{-\gamma R}\left(1 + \gamma R + \frac{4}{9}\gamma^2 R^2 + \frac{1}{9}\gamma^3 R^3\right)\right] \qquad (14)$$

where the solution neglects displacement currents. From Equations 11 and 12, $\gamma R = \sqrt{2i}\,B$, and Equation 14 is seen to be solely a function of B when normalized to the primary field intensity. The quadrature (Q) and inphase (I) components of Equation 14 in the small induction number limit ($B << 1$) have the following magnitude relationships (Kaufman and Keller 1983)

$$I(H_{tz}) \quad H_{pz} + I(H_{sz}) \qquad (15)$$

$$I(H_{sz}) << Q(H_{tz}) << H_{pz} \qquad (16)$$

$$Q(H_{tz}) \approx Q(H_{sz}) \qquad (17)$$

and

$$Q\left(\frac{H_{sz}}{H_{pz}}\right) \approx \frac{B^2}{2} = \frac{\sigma\mu\omega R^2}{4} \qquad (18)$$

28. Equation 18 indicates that if an EM system operates within the limits of the small induction number approximation, satisfies the other criteria specified for the loop-loop systems under consideration, and can be calibrated and designed to measure $Q(H_{sz}/H_{pz})$, then

$$\sigma \approx \left(\frac{4}{\mu\omega R^2}\right) Q\left(\frac{H_{sz}}{H_{pz}}\right) \qquad (19)$$

i.e., the conductivity of the homogeneous earth can be determined directly. If the earth is not homogeneous, the value determined from Equation 19 is properly termed an apparent conductivity (σ_A) in the same sense as an apparent resistivity determined, say, with a Schlumberger array and using the homogeneous half-apace geometric factor.

EM Sounding Interpretation

29. A set of EM sounding data is collected by making field measurements at increasing Tx-Rx separations, at decreasing transmitter frequencies, or both. The measured data can be converted to field strengths and phases and plotted as a function of R , f , B , or some other parameter. For a small induction number sounding system, the data can be converted directly to apparent conductivity using a relation such as Equation 19; apparent conductivity data are then plotted as a function of R or B . Interpretation of the sounding data in terms of a multilayer earth model is then accomplished by comparison with standard curves or by use of an inversion computer program.

30. Although extensive catalogs of standard curves for EM sounding do not exist in published form, forward computer modeling techniques for a variety of EM systems and layered earth models are available. For the small induction number, loop-loop sounding system, forward EM modeling of a given layered earth model is greatly simplified. The simplification results from the fact that the behavior exemplified by Equation 19 arises for the case where the induced currents in the earth are not magnetically coupled, i.e., the interaction between horizontal current rings is negligible. Thus, the contributions of the horizontal currents in each subsurface layer can be computed and summed directly with no consideration of interactions. The procedure for determining a model sounding curve will be addressed in Part IV of this report.

PART III: ELECTROMAGNETIC SURVEYING FOR GROUND WATER

Concepts

31. Neither the CW EM methods considered in this report nor the rapidly developing transient or time-domain EM methods can be regarded as major conceptual breakthroughs in ground-water exploration and detection. Ideally, a properly conducted and interpreted EM survey should yield the same information as a properly conducted and interpreted resistivity survey, i.e., the horizontal or vertical variation or conductivity/resistivity with distance or depth, respectively. The horizontal or vertical conductivity profile must then be interpreted in terms of a hydrogeological model, using any additional complementary data, such as other geophysical survey results, borehole data, and specific or general geological information about the area. Confidence in interpretation of the EM data, as with any geophysical method, will increase as the amount and quality of complementary data increase.

32. From the above discussion, it is clear that the EM techniques are not "stand-alone" ground-water detection methods; however, the EM techniques do offer several significant advantages over the electrical resistivity method, for example, in a ground-water detection program:

a. In arid regions it is often difficult to conduct electrical resistivity surveys due to high electrode contact resistance. With the loop transmitter EM techniques, high near-surface resistivities pose no problems, since subsurface coupling is achieved inductively, requiring no surface contact.

b. For a given maximum depth of investigation, EM surveys proceed more rapidly and with considerably less manpower than electrical resistivity surveys. If a 180-m (~600-ft) depth of investigation is required, an electrical resistivity array ~1,500 m (~5,000 ft) long is required (distance between outer electrodes in a Schlumberger array for the last measurement in the sounding), while the same depth of investigation can commonly be achieved with an interloop spacing of 180 to 360 m in a CW EM survey or a 180-m-square transmitter loop in a transient EM system.

c. From b, the logistical complexity of conducting an EM survey is seen to be less than for an electrical resistivity survey. Also, it is possible to mount transmitter and receiver loops on separate vehicles and conduct vehicle-mounted EM surveys in some cases.

d. Since the Tx-Rx spacing in EM surveying is considerably smaller than the electrode spacing in resistivity surveying, the EM

measurements are much less susceptible to the erratic readings and errors caused by lateral conductivity variations. This also implies that the EM techniques will have better resolution in horizontal profiling than the resistivity method.

Some disadvantages of a specific small induction number, loop-loop CW EM system will be discussed in Part IV.

33. From the above considerations, three possible applications are envisioned for the CW EM systems in ground-water detection programs: (a) to replace electrical resistivity in a complementary geophysical methods approach to ground-water detection (see paragraph 6), (b) to be used in conjunction with electrical resistivity and seismic refraction, or (c) to conduct both vertical sounding and horizontal profiling at a site in a single-method approach. The second application of the CW EM systems would allow rapid horizontal profiling about a single location or between two locations at which seismic refraction and resistivity surveys are conducted; this procedure would allow a ground-water detection program to approach an exploration program without significantly increasing the field effort or productivity.

34. Results of geophysical surveys are interpreted using geophysical models that are consistent with the survey data. Hydrogeological models are then deduced from the geophysical models. This procedure is subjective, and the resulting hydrogeological models are not unique. The subjectivity and nonuniqueness decrease as the information available to constrain the models increases. Some typical hydrogeological models are illustrated in Figure 4. Although other models are possible to describe natural ground-water occurrences, these are the models most frequently invoked to explain geophysical results and models. Knowledge of the geology of the area in question may eliminate some of the models in Figure 4 from consideration. For the geophysical ground-water detection mode, where the geophysical surveys are conducted at one location, the hydrogeological models will be one-dimensional, such as shown in Figures 4a, 4b, and 4c, even though a more complex model, such as Figures 4d, 4e, and 4f, may be suspected. An exploration program such as suggested in paragraph 33, including horizontal profiling, is required before models such as shown in Figures 4d, 4e, and 4f can be invoked to explain geophysical results.

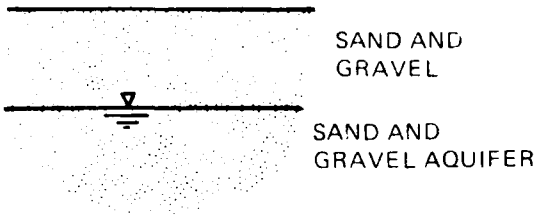

a. Unconfined aquifer model

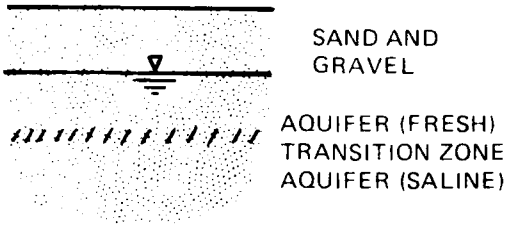

b. Unconfined aquifer model with transition to saline ground-water conditions

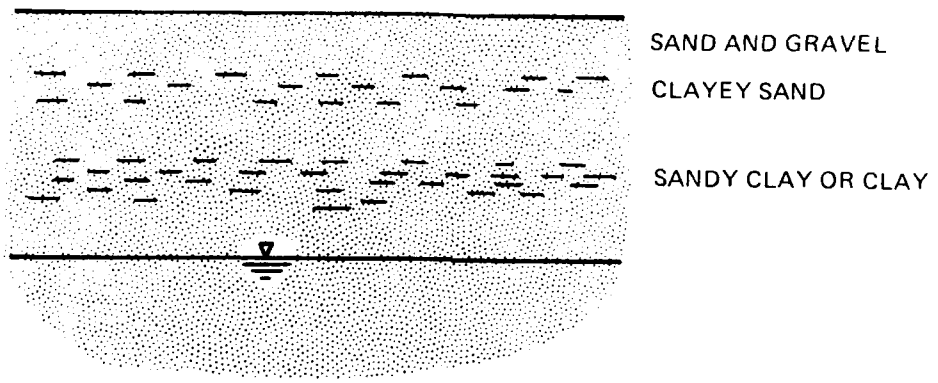

c. Unconfined aquifer model with sandy clay or clayey sand above the water table

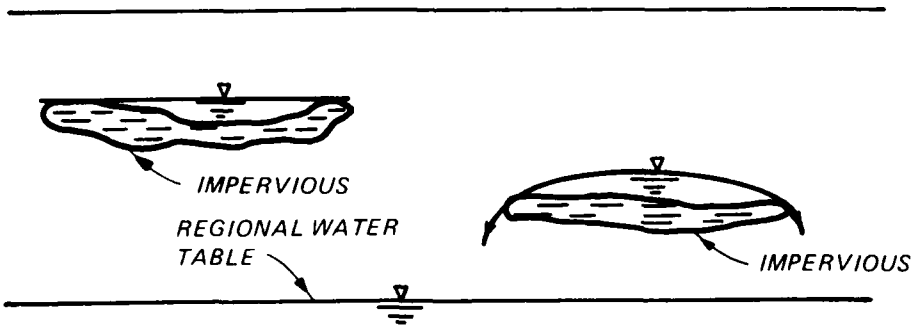

d. Perched water tables model

Figure 4. Typical hydrogeological models used to explain geophysical results (Continued)

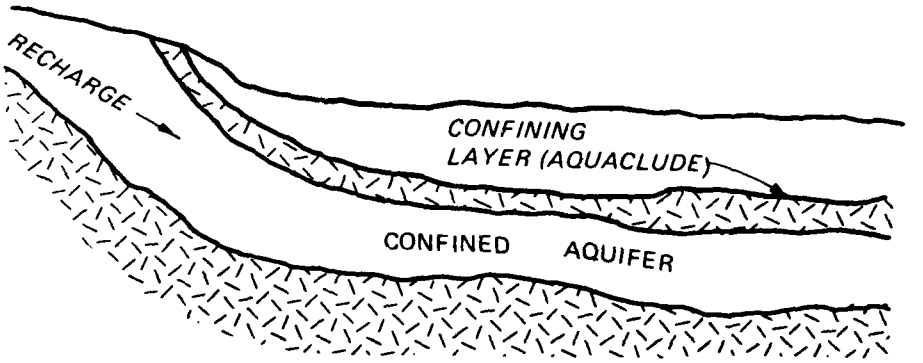

e. Confined aquifer model

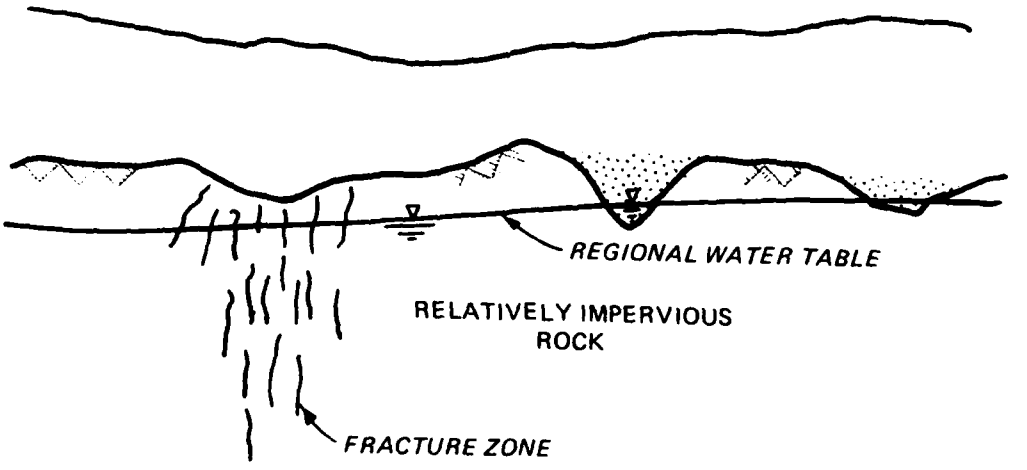

f. "Fracture zone aquifer" model

Figure 4. (Concluded)

Review of Selected Previous Studies

35. Electromagnetic Surveys, Inc., (EMSI 1979) discusses the results of a numerical modeling study of horizontal loop EM sounding for ground-water exploration. The modeled EM system consists of a 5-m-radius horizontal loop transmitter, a three-component magnetic field detector receiver, and Tx-Rx spacings ranging from 100 to 2,000 m. The magnitude and phase of the vertical and radial magnetic field, the ellipticity, and the tilt angle responses of selected geohydrological models are calculated for transmitter frequencies from 0.1 to 1,000 Hz. Four hydrogeological models are considered which are common in the Central Valley of California: (a) basal freshwater-saltwater boundary (Figure 4b), (b) deeply buried freshwater aquifer, (c) perched saltwater lenses, and (d) surface clay layer over freshwater aquifer. The only model that is not definable with the above hypothetical EM system is the deeply buried freshwater (resistive) aquifer; for Tx-Rx spacings of 500 and 2,000 m, a 30-m-thick freshwater aquifer is not detectable below the 100-m depth. The perched saltwater lens and surface clay layer models are easily definable by the EM system.

36. Ryu, Morrison, and Ward (1972) conducted horizontal loop EM sounding experiments across the Santa Clara Valley, Calif., using a 10-m-radius, 20-turn horizontal transmitter loop, 122 and 214 m Tx-Rx separations, and 14 transmitter frequencies between 200 Hz and 10 kHz. The results of the EM interpretations are consistent with well data and electrical resistivity soundings. The EM soundings successfully detected and mapped a resistive freshwater aquifer, consisting of sands and gravels, surrounded by clays. The aquifer is about 18 m thick with the top at a depth of about 8 m in the central part of the valley. The results are consistent with the results of the EMSI numerical study.

37. The two preceding studies (EMSI 1979; Ryu, Morrison, and Ward 1972) did not specifically address the case of small induction number soundings, in fact the second study had induction numbers in the range of $0.1 < B < 10.0$. Also, these studies concerned EM sounding exclusively. Palacky, Ritsema, and De Jong (1981) give results of EM horizontal profiling surveys for groundwater exploration under conditions that satisfied the small induction number criterion. The primary targets of the EM surveys were fracture zones in a

resistive granitic basement rock (see Figure 4f). Except in the fracture zones, water wells in the granite are unproductive. In some cases, the fractures can be detected as lineaments on aerial imagery but cannot be recognized visually at ground level. However, siting wells based on aerial imagery interpretation is unsatisfactory in this case, since location errors of ~5 m can mean the difference between dry holes and productive wells. The horizontal loop EM profiling technique proved to be extremely successful in locating the fracture zones. Figure 5 from Palacky, Ritsema, and De Jong (1981) shows the results of horizontal loop EM profiling (HLEM), VLF profiling,* and resistivity profiling. Based on this investigation, two conclusions are noteworthy: (a) the EM methods are more sensitive to the targets than resistivity, and (b) even making measurements at three frequencies and with 10-m measurement intervals, the HLEM surveys require less time than resistivity surveys with 20-m measurement intervals and require two operators compared to a three- or four-man party for resistivity. The authors report that, at the time of preparing the case history (1981), 24 wells had been sited based on HLEM profiling and 23 were productive.

38. The small induction number loop-loop EM system used in the present field studies and described in Part IV has been used extensively for mapping contaminant plumes at landfill and hazardous waste sites (e.g., McNeill 1982; Greenhouse and Slaine 1983; Sweeney 1984) and in some cases for detecting and mapping saltwater intrusion into freshwater aquifers (Stewart 1982). For these applications, the small induction number EM techniques work exceptionally well. Generally, the objectives in these studies are to map anomalous zones associated with the contaminant plumes or saltwater intrusion; other than noting general agreement with results of other geophysical techniques and ground-water monitoring wells, the interpretations are mostly limited to qualitative assessments. Stewart (1982), however, gives examples of quantitative interpretations of soundings which agree with known conditions; he concludes that the quantitative interpretations are possible only when the geological conditions can be reasonably approximated with a two-layer model.

---

* VLF is a far-field EM technique using distant radio transmitters as EM sources.

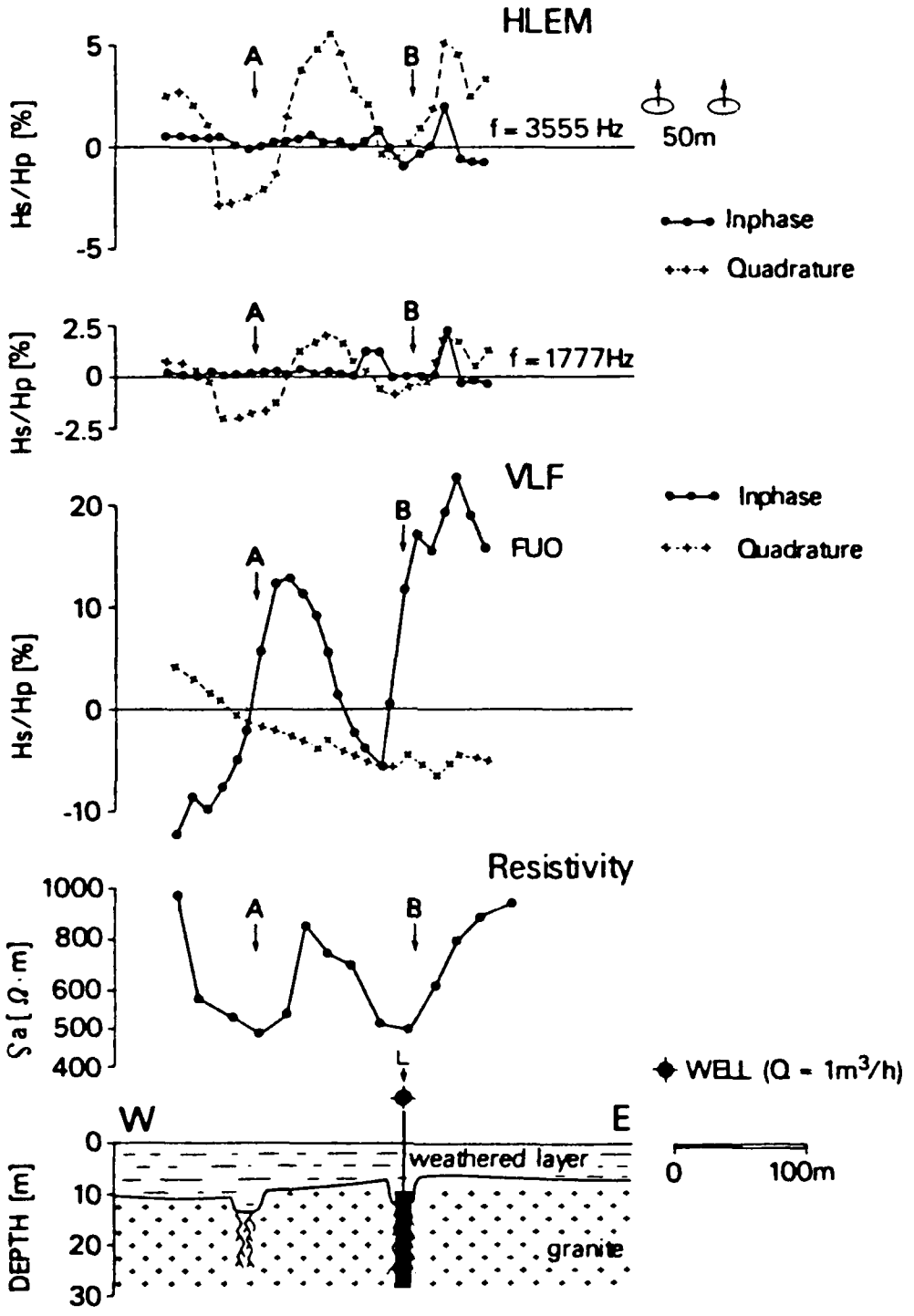

Figure 5. Results of three geophysical measurements obtained in a target area near Rapadama, Republic of Upper Volta (now Burkina Faso). From the top, HLEM at two frequencies, VLF (FUO transmitter) and Schlumberger resistivity profiling (AB = 200, MN = 40 m). Two conductors, A and B, were identified by the three methods. Drilling of the conductor B revealed a productive aquifer (from Palacky, Ritsema, and De Jong 1981)

PART IV: FIELD INVESTIGATIONS

EM Equipment and Interpretation Principles

Equipment description

39. The loop-loop, small induction number, CW EM system selected for the field studies, known as the EM 34,* is described by McNeill (1980a,b; 1982). The EM 34 is a two-man portable system consisting of separate transmitter and receiver consoles and 0.63-m-diam transmitter and receiver loop** (magnetic dipole) antennae. Figure 6 shows the EM 34 in use at Fort Carson. Total weight of the system is approximately 20 kg.

40. The EM 34 transmitter operates at switch-selectable, controlled frequencies of 6,400 Hz, 1,600 Hz, and 400 Hz, and each frequency is keyed to Tx-Rx spacings of 10, 20, and 40 m, respectively. For the range of conductivities considered in Part II, the operating induction numbers for this system are tabulated below.

	Induction Number (B)		
Conductivity σ (mho/m)	f = 6,400 Hz R = 10 m	f = 1,600 Hz R = 20 m	f = 400 Hz R = 40 m
10^{-3}	0.04	0.0001	0.00003
10^{-2}	0.01	0.003	0.0008
10^{-1}	0.4	0.1	0.03
10^{0}	13	3.2	0.8
10^{1}	400	100	26
10^{2}	13,000	3,200	800

The values of $B < 1$ are above the dotted line in the tabulation, and in general the small induction number condition is satisfied only for $\sigma \leq 0.1$ mho/m or $\rho > 10$ ohm-m for the EM 34 system. This implies that the EM 34, which is calibrated to read directly in conductivity units (mmho/m), has a limited dynamic range. As shown in Figure 7, the approximate linear relation implied by Equation 19 between detected signal and conductivity begins to seriously break down for $\sigma > 0.1$ mho/m . The linearity breakdown is more serious for

---

* Manufactured by Geonics Limited, Mississauga, Ontario, Canada.

** Common terminology defines the separate transmitter (or receiver) and its antenna as the small loop transmitter (or receiver). However, the reader should be aware that the transmitter (or receiver) and small loop (antenna) are separate hardware items and physically separated from each other during field measurements.

a. The EM 34 in use at Fort Carson

b. Close-up of the EM 34 receiver

Figure 6. The two-man portable EM 34 CW EM system

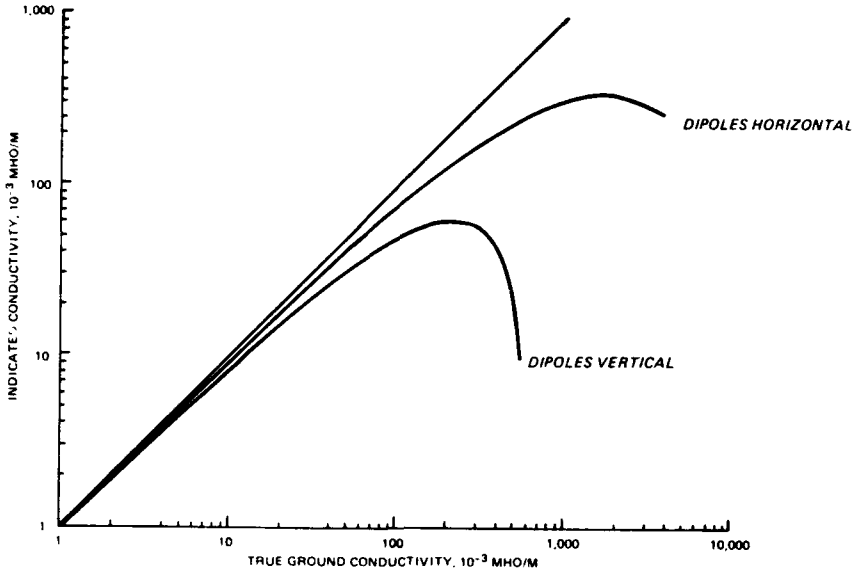

Figure 7. Plot of indicated versus true conductivity for the EM 34 over a uniform half-space

the case of horizontal coplanar loops (vertical dipoles) than for vertical coplanar loops (horizontal dipoles). For very low conductivity (σ < 0.001/mho/m), signal levels are too small to be detected.

41. A reference cable links the transmitter and receiver consoles, and a null meter indicates when the selected Tx-Rx spacing is reached. At each coil spacing, conductivity measurements can be made with both coils horizontal, i.e., vertical dipoles (V), or with vertical coplanar coils, i.e., horizontal dipoles (H). If the earth were uniform vertically and laterally, the vertical and horizontal dipole orientations would both indicate the same apparent conductivity, which in this case would equal the true conductivity (subject to the limitations shown in Figure 7). In general, however, for a layered earth case, the apparent conductivities indicated with the V and H dipole configurations will be different, since the effective depths of investigation are different. With two coil configurations and three Tx-Rx spacings, it is possible to obtain six apparent conductivity values with the EM 34 centered at a given surface point.

Interpretation principles

42. For the layered earth case, calculation of the small induction number EM response, for cases where the layer thicknesses are also small with respect to the skin depth, is characterized by its remarkable simplicity, when

compared to other EM methods and electrical resistivity methods. For an N-layered model with layer conductivities σ_1 and thicknesses h_i, the quadrature component of H_{sz} on the surface at a distance R from a vertical magnetic dipole m is given by (Kaufman and Keller 1983)

$$Q(H_{sz}) = \frac{\mu\omega m}{16\pi R} \sum_{i=1}^{N} \sigma_i G_{zi}^{V} \tag{20}$$

where the G_{zi}^{V} are purely geometric factors. The geometric factors take the general form

$$G_{zi}^{V} = \frac{R}{\sqrt{4z_{it}^2 + R^2}} - \frac{R}{\sqrt{4z_{ib}^2 + R^2}} \tag{21}$$

where z_{it} and z_{ib} are the depths to the top and bottom, respectively, of the i^{th} layer, i.e.,

$$z_{it} = h_1 + h_2 + \ldots + h_{i-1}$$

and

$$z_{ib} = h_1 + h_2 + \ldots + h_{i-1} + h_i$$

For layer 1

$$G_{z1}^{V} = 1 - \left(\frac{R}{\sqrt{4h_1^2 + R^2}} \right)$$

and, for layer N (assumed to be infinite in depth extent),

$$G_{zn}^{V} = \frac{R}{\sqrt{4\left(\sum_{1}^{n-1} h_i\right)^2 + R^2}}$$

43. The simplicity inherent in Equation 20 makes it straightforward to compute apparent conductivity curves for layered earth models. Using the appropriate geometric factors for the horizontal dipole orientation $\left(G^H_{zi}\right)$, horizontal dipole as well as vertical dipole sounding curves (as a function of R , the Tx-Rx spacing) can be generated easily. The simplicity of the response calculations results from the fact that current in individual subsurface layers is entirely horizontal (in the absence of significant lateral variations) and that interactions between eddy current loops can be neglected for small induction numbers.

44. McNeill (1980a) defines cumulative response functions $R^V_z\left(\frac{z_j}{R}\right)$ and $R^H_z\left(\frac{z_j}{R}\right)$ for the vertical and horizontal dipole orientations, respectively. These response functions describe the relative contribution to the secondary magnetic field from all material below depth z_j at Tx-Rx spacing R . Function $R^V_z\left(\frac{z_j}{R}\right)$, for example, is related to the geometric factors in the following manner

$$R^V_z\left(\frac{z_j}{R}\right) = \frac{R}{\sqrt{4z_j^2 + R^2}} \tag{22}$$

and

$$G^V_{zi} = R^V_z\left(\frac{z_{it}}{R}\right) - R^V_z\left(\frac{z_{ib}}{R}\right) \tag{23}$$

Figure 8 illustrates the behavior of R^V_z and R^H_z , where Z is the normalized depth $\frac{z_i}{R}$. It is clear from Figure 8 that the "depth of investigation" is greater for the vertical dipole orientation than for the horizontal dipole orientation. For example, 70 percent of the response at the surface is due to material shallower than 0.75 R for the horizontal dipole case and 1.5 R for the vertical dipole case. For the EM 34 system, this is the origin of the rules of thumb that the depths of investigation for the three Tx-Rx spacings (R = 10, 20, and 40 m) are 15, 30, and 60 m (1.5 R) for the vertical dipole case and 7.5, 15, and 30 m (0.75 R) for the horizontal dipole case. Utility of the rules of thumb, as well as theoretical response curves based on

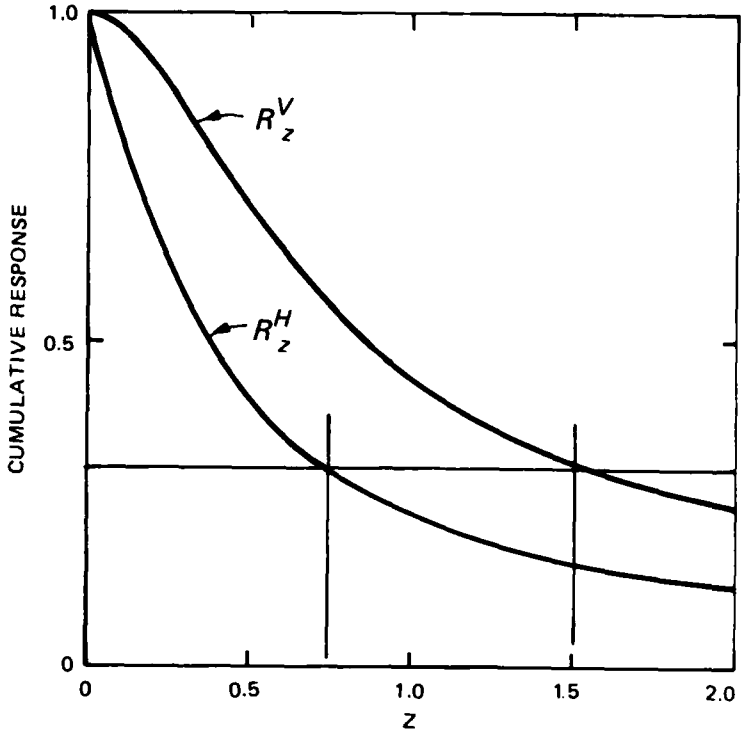

Figure 8. Cumulative response versus depth for vertical and horizontal dipoles

Equations 20-23, will be examined later in this part.

45. The simplicity of the response calculations makes it easy to predict the ideal apparent conductivity measurement values of the EM 34 for any postulated geologic cross-sectional model. Figure 9, for example, gives the equations for computing apparent conductivity for two-, three-, and four-layer models using the R_z^V function. For a given Tx-Rx spacing, the apparent conductivity values along a profile line over a multilayered model with lateral variations in thickness can be computed for comparison with field data. Also, for a given multilayered model, the apparent conductivity values for the three Tx-Rx spacings and the two coil orientations can be calculated to give theoretical sounding curves. The calculated sounding curves can be compared to field EM 34 data in much the same way as resistivity interpretation using master curves. In practice, interpretation of EM 34 sounding data is limited to cases where the subsurface closely approximates two layers, due to the small number (six) of data points (McNeill 1980a,b, 1982; Stewart 1981).

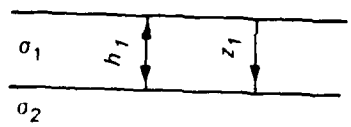

$$\sigma_A = \sigma_1 \left[1 - R_z^V\left(\frac{z_1}{R}\right)\right] + \sigma_2 R_z^V\left(\frac{z_1}{R}\right)$$

a. Two-layer model

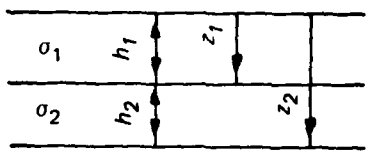

$$\sigma_A = \sigma_1 \left[1 - R_z^V\left(\frac{z_1}{R}\right)\right] + \sigma_2 \left[R_z^V\left(\frac{z_1}{R}\right) - R_z^V\left(\frac{z_2}{R}\right)\right] + \sigma_3 R_z^V\left(\frac{z_2}{R}\right)$$

b. Three-layer model

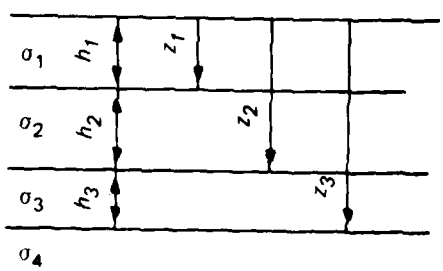

$$\sigma_A = \sigma_1 \left[1 - R_z^V\left(\frac{z_1}{R}\right)\right] + \sigma_2 \left[R_z^V\left(\frac{z_1}{R}\right) - R_z^V\left(\frac{z_2}{R}\right)\right] + \sigma_3 \left[R_z^V\left(\frac{z_2}{R}\right) - R_z^V\left(\frac{z_3}{R}\right)\right] + \sigma_4 R_z^V\left(\frac{z_3}{R}\right)$$

c. Four-layer model

Figure 9. Apparent conductivity relations for two-, three-, and four-layer models

Review of Field Sites and Previous Geophysical Results

46. The White Sands, N. Mex., and Fort Carson, Colo., field test sites are discussed in Report 6 of this series (Butler and Llopis 1984). Characteristics of the sites will be briefly reviewed here. Figure 10 shows the five field test locations at White Sands. Water table depths, water quality data, and the amount and type of available geological information, as summarized in Table 1, are quite varied. The water tables occur in unconsolidated sediments in all five locations. Geophysical models deduced from the seismic refraction and electrical resistivity surveys at the White Sands locations are shown in Figure 11. Table 2 presents the ground-water assessments for the five locations based on a hydrogeological model interpretation of the geophysical models in Figure 11. Finally, Table 3 compares the predicted and measured water table depths. The predicted water table depths are consistently shallower than the measured water table depths. For SW-19 and MAR, the shallower predicted water table depths are not unreasonable due to possible drawdown at the well measurement point; this explanation does not hold for B-30 and T-14, however, and the results for HTA-1 must be regarded as a failure of the ground-water detection procedure.

47. At Fort Carson, a location was selected near a well that produces fresh water from the Dakota Sandstone aquifer (see Figure 12). Figure 13 is a geological cross section based on the depth to the Dakota Sandstone (~82 m) at the well location and the average regional dip (~63 m/km) to the east (Dardeau and Zappi 1977). The Dakota Sandstone is underlain and overlain by shales, which serve as aquacludes and produce artesian conditions. The geophysical survey results suggest and a recent US Geological Survey report (Leonard 1984) confirms that the actual geological conditions at the site may not be exactly as shown in Figure 13. Alternatives to the situation as shown in Figure 13 will be introduced later in this part. Also shown in Figure 13 are geophysical models developed for one survey location at Fort Carson; the original geological interpretation in Butler and Llopis (1984) associated the velocity interface at approximately 10-m depth (~1,680 m NGVD) with the top of the Dakota Sandstone; however, this will be reassessed.

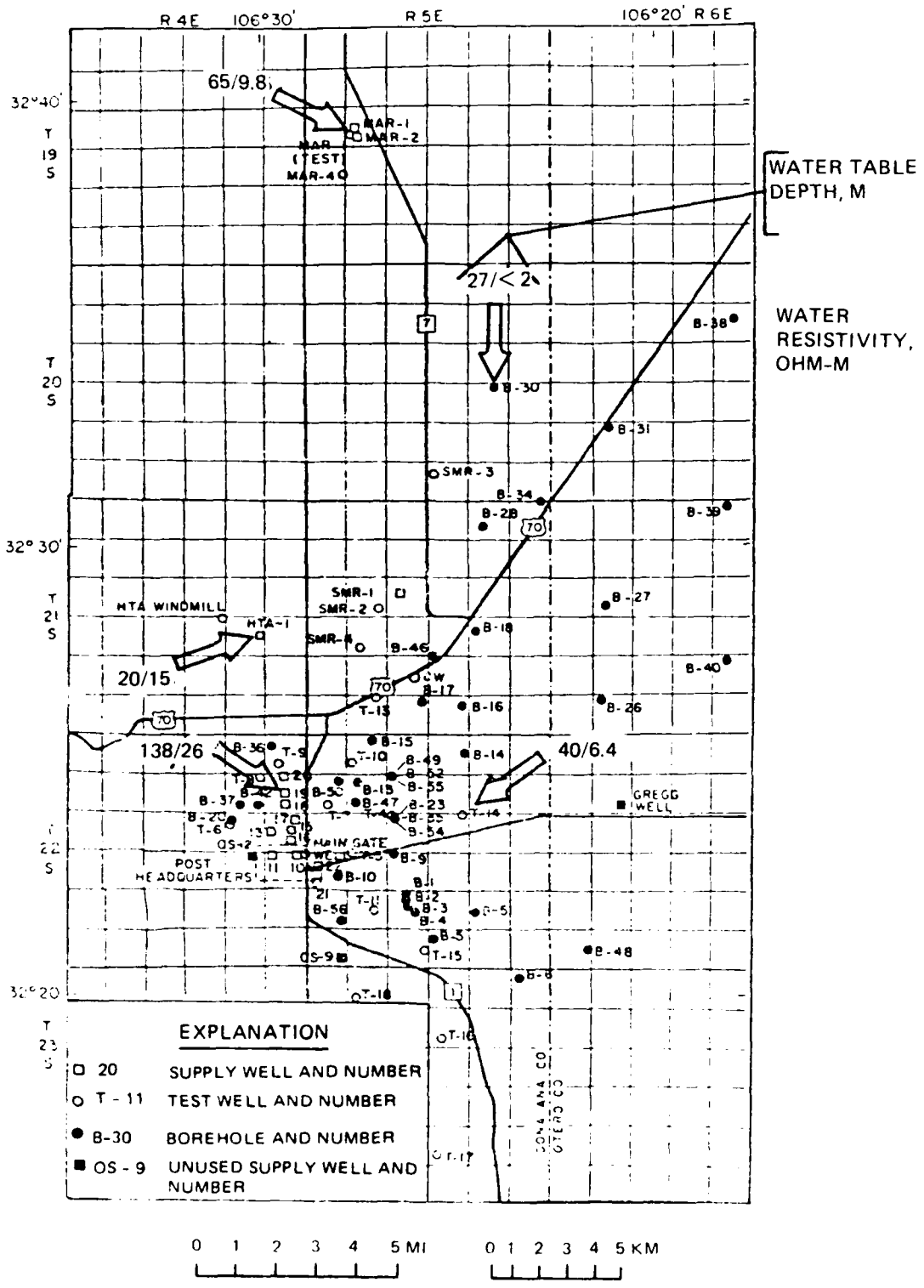

Figure 10. Geophysical survey locations--White Sands Missile Range, N. Mex. Data presented for each site include water table depth (metres) and water resistivity (ohm-metres) (from Cruz 1981)

Table 1

Summary of Geologic/Ground-Water Information

for White Sands Test Locations

Location	Measured Water Table: Depth, m (Date)	Measured Water Table: Variation m	Resistivity, ohm-m (Water Quality*)	Type of Geologic Information Available and Summary	Comments
HTA-1	19.5 (15 Feb 83)	1.8	15 (fresh)	Limited borehole lithology information. Sand and gravel to 25 m. Weathered granite encountered at 25 m.	Natural gamma and neutron borehole geophysical logs
B-30	27.3 (15 Feb 83)	0.3	<1 (@ 56.4 m) (saline)	None	Natural gamma and neutron borehole geophysical logs
T-14	40.2 (16 Feb 83)	0.3	6.4 (@ 61 m) 6.7 (@ 91 m) (marginal)	Borehole lithology log for entire 1,829-m depth. Sand with silt and clay, 0-32 m; clay with sand and silt, 32-36 m; sand with clay, 36-55 m; clay with sand and silt, 55-131 m.	Complete set of borehole geophysical logs from 122-1,829 m

(Continued)

* Generally, fresh water is considered to have <1,000 mg/ℓ total dissolved solids. This criterion converts approximately to a "specific conductance" of <1,560 μmhos/cm or a resistivity of >6.4 ohm-ft.

Table 1 (Concluded)

Location	Measured Water Table: Depth, m (Date)	Measured Water Table: Variation m	Resistivity, ohm-m (Water Quality*)	Type of Geologic Information Available and Summary	Comments
MAR	65.2 (MAR-2; 14 Feb 83) 67 (MAR-2; 1981)	0.3	10 (~90 m) 0.2 (@228 m in MAR-2 and MAR-3) (fresh @90 m)	Borehole lithology log. Gravel, 0-34 m; clay, 34-49 m; gravel, 49-50; clay, 50-61; gravel, 61-63; clay, 63-69; etc.; predominantly clay below 192 m.	Electric logs available
SW-19	138.4 (25 Feb 83) 130.1 (for SW-18) 156.7 (for SW-20)	1.5	25 (>122 m) (fresh)	Limited material descriptions. Poorly sorted sands and gravels to >274 m.	Nonpumping water level; 124.9 m (22 Jul 64) (122.5 m, SW-18; 140.8 m, SW-20)

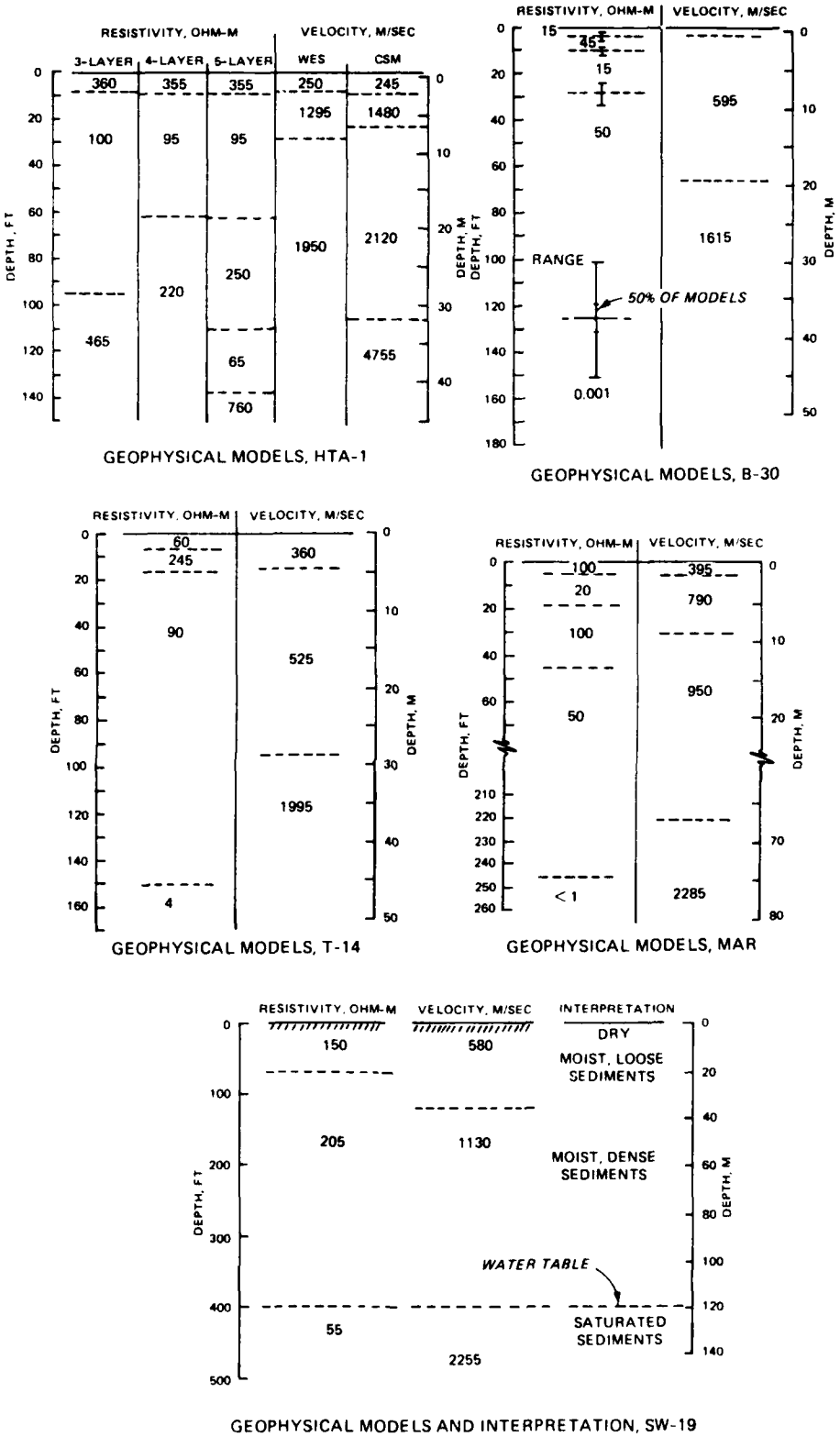

Figure 11. Geophysical models for five White Sands locations (from Butler and Llopis 1984)

Table 2

Summary of White Sands Geophysical Ground-Water Assessments

Location	Predicted Water Table Depth, m	Water Quality	Predicted Aquifer Thickness, m	Confidence in Ground-Water Assessment
HTA-1	2.4	Fresh	30.5	Poor
B-30	19.8	Fresh from 19.8-38.1 m, becoming very saline below 38.1 m	?	Fair to good
T-14	29.0	Fresh from 29-46 m, becoming saline below 46 m	?	Poor to fair
MAR	48.8	Fresh from 48.8-91.4 m; very saline from 91.4-305 m	Base of aquifer, 305 m	Fair
SW-19	122.0	Fresh	?	Very good

Table 3

Comparison of Predicted and Measured Water Table Depths

Location	Predicted Depth D_p	Measured Depth D_m	Percent Error $\frac{D_m - D_p}{D_m} \times 100$	Required Percent Increase in D_p - $\frac{D_p - D_m}{D_p} \times 100$
HTA-1*	2.4*	19.5	88*	700*
B-30	19.8	27.3	27	38
T-14	29.0	40.2	28	39
MAR	48.8	65.2	25	34
SW-19	122.0	138.4	12	14

* Discussion of error for the HTA-1 case is not meaningful since the water table was not detected by the complementary geophysical methods.

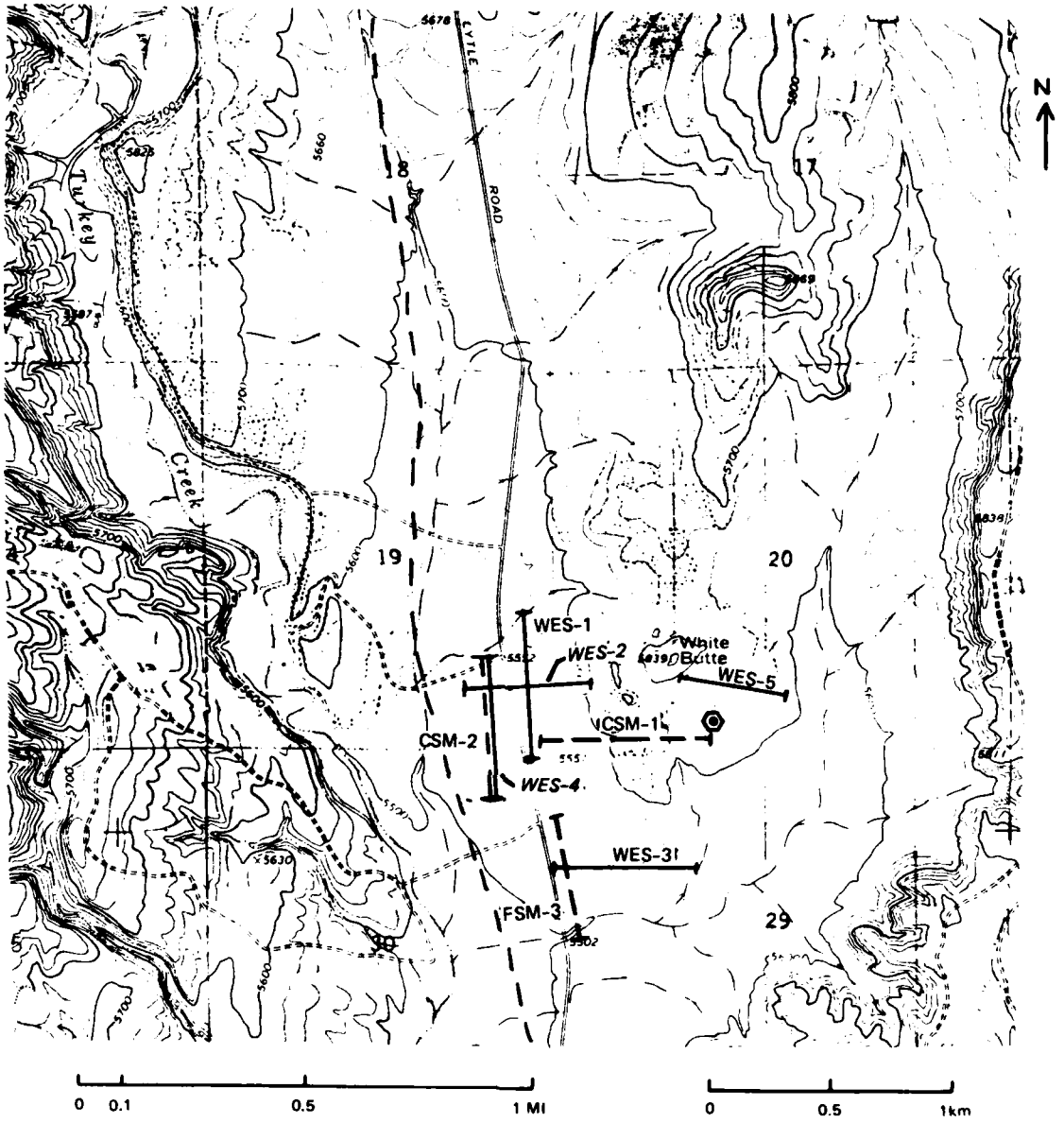

Figure 12. Fort Carson survey layout: EM--electromagnetic survey, current study; CSM--seismic refraction survey; WES--electrical resistivity sounding (from Butler and Llopis 1984)

EM Survey Results and Analyses: White Sands, N. Mex.

Field procedures

48. At four of the White Sands location (MAR, HTA-1, T-14, and B-30), two EM soundings were conducted at the locations of the previous geophysical

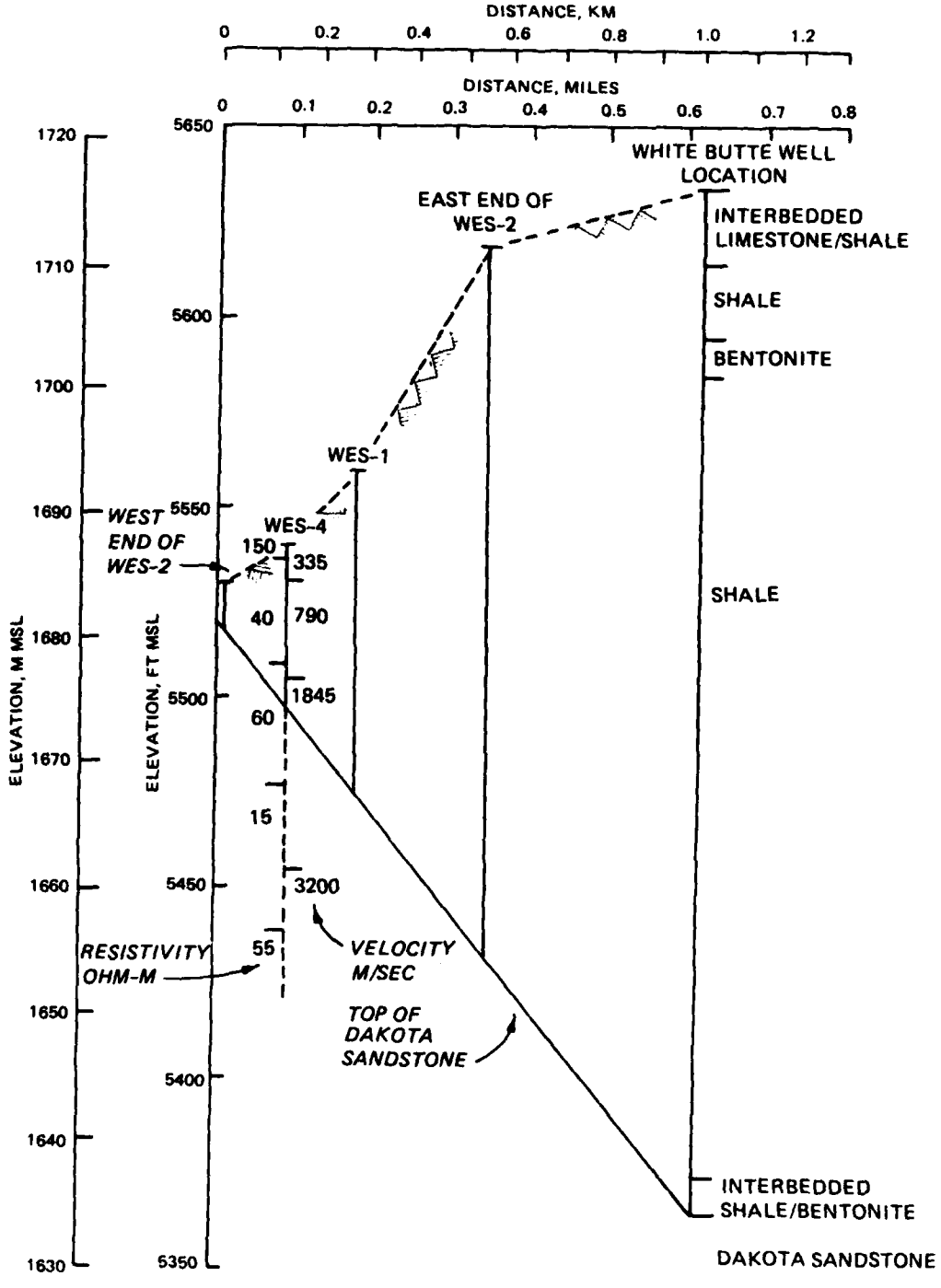

Figure 13. Cross section of Fort Carson site, showing surface topography, top of the Dakota Sandstone, survey line locations, White Butte well borehole log, and WES-4/CMS-2 geophysical models

surveys. The two sounding lines were perpendicular to each other at the midpoints, and the three possible Tx-Rx spacings and two coil orientations were used for each sounding. Results of the two soundings were averaged to give the sounding data for each site. At SW-19, only one sounding was conducted.

Field data

49. Results of the EM 34 field survey are given in Table 4, where lines I and II refer to the perpendicular sounding directions at each site, and line I is generally parallel and along the line of the previous resistivity and refraction surveys at the site. From Figure 7 it is evident that some of the field data, particularly for B-30 and T-14, have apparent conductivities that are high enough to require correction for nonlinearity of equipment response. The data in Table 5 have been corrected using the relations in Figure 7 and represent the average of soundings I and II for each case.

Assessment of depth of investigation rules of thumb

50. Figures 14-18 present the EM 34 data from Table 5 as sounding curves of apparent conductivity versus depth of investigation, using the 0.75 R and 1.5 R rules of thumb for depths of investigation for the vertical (V) and horizontal (H) dipole orientations, respectively. Superimposed are the layered model interpretations of electrical resistivity soundings (converted to conductivity) for the same locations (Butler and Llopis 1984). The rules of thumb result in two identical depths of investigation at 15 and 30 m for the V and H dipole orientations. Clearly, the four depth points resulting from the rules of thumb are incapable of providing anything more than a general trend of conductivity with depth.

51. Measured conductivities for the ten 15- and 30-m depths of investigation data values for the V and H dipole orientations differ by amounts varying from 0 percent to nearly 100 percent. Three values differ by <10 percent, five values differ by ~20 to 30 percent, and two values differ by >50 percent. For the low-conductivity locations (HTA-1 and SW-19), the V dipole measured conductivities are consistently larger than the H dipole conductivities. For the higher conductivity locations (B-30, T-14, and MAR), the comparisons between the V and H measured conductivities are inconsistent.

52. Using the rules of thumb for depth of investigation, all of the EM 34 sounding curves fall within ranges generally consistent with the models

Table 4

EM 34 Sounding Results, White Sands, N. Mex.

Location	Sounding	Coil Spacing m	Apparent Conductivity, mmho/m V (Vertical Dipoles)	Apparent Conductivity, mmho/m H (Horizontal Dipoles)
HTA-1	I	10	9.1	6.9
		20	7.5	6.2
		40	30 (noisy)	7
	II	10	10	9.5
		20	9.3	9.2
		40	12 (noisy)	7.5
B-30	I	10	34	39
		20	53	54
		40	66	75
	II	10	37	39
		20	55	50
		40	72	71
T-14	I	10	45	37
		20	26	39
		40	17.5	40
	II	10	48	38
		20	30	48
		40	16	42
MAR	I	10	14.5	19
		20	6.8	16
		40	14	15
	II	10	22	28.5
		20	11.5	27
		40	13.5	25.5
SW-19	I	10	10.5	8.1
		20	9.6	7.6
		40	8.8	7.5

Table 5

Corrected and Averaged EM 34 Sounding Results

White Sands, N. Mex.

Location	Coil Spacing m	Apparent Conductivity mmho/m		Apparent Resistivity ohm-m	
		V	H	V	H
HTA-1	10	9.6	8.2	83	122
	20	8.4	7.7	100	130
	40	15	7	67	143
B-30	10	60	48	17	21
	20	120	65	8	15
	40	Very large	98	~0	10
T-14	10	95	45	11	22
	20	45	54	22	19
	40	23	50	43	20
MAR	10	25	28	40	36
	20	11	25	91	40
	40	18	23	56	43
SW-19	10	10.5	8.1	77	123
	20	9.6	7.6	83	132
	40	8.8	7.5	95	133

deduced from the resistivity soundings. Comparison of results from B-30 and T-14 (Figures 15 and 16), however, illustrates the shortcomings of the rules of thumb, which are completely independent of the geoelectric sections. For example, the EM 34 response at B-30 seems to be totally dominated by the EM response of the very high-conductivity "basement" at the 38-m depth; i.e., the 30-m-thick, 20-mmho/m layer above the basement is transparent to the EM 34. However, the EM 34 apparently does not exhibit a response at T-14 to the 82 mmho/m basement at a depth of 47 m beneath a 30-m-thick, 4-mmho/m layer. With the exception of the R = 40 m intercoil spacing for the V dipole orientation, the EM 34 data seem to qualitatively indicate variations between the five locations in the "average conductivity" above the rule-of-thumb depth of investigation. Thus, these data support the concept that the EM 34 could be

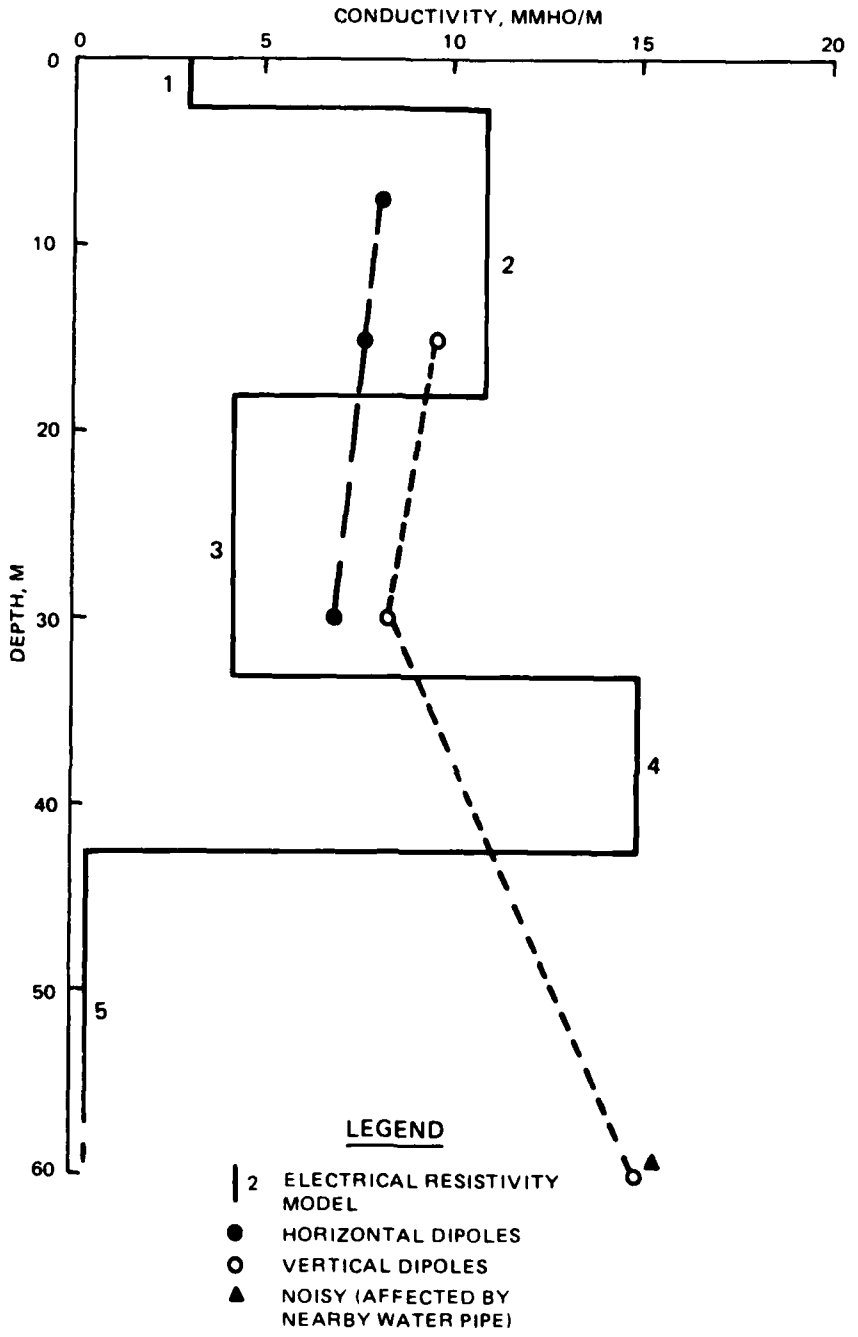

Figure 14. EM 34 data plotted at rules-of-thumb depths of investigation compared to electrical resistivity model for HTA-1

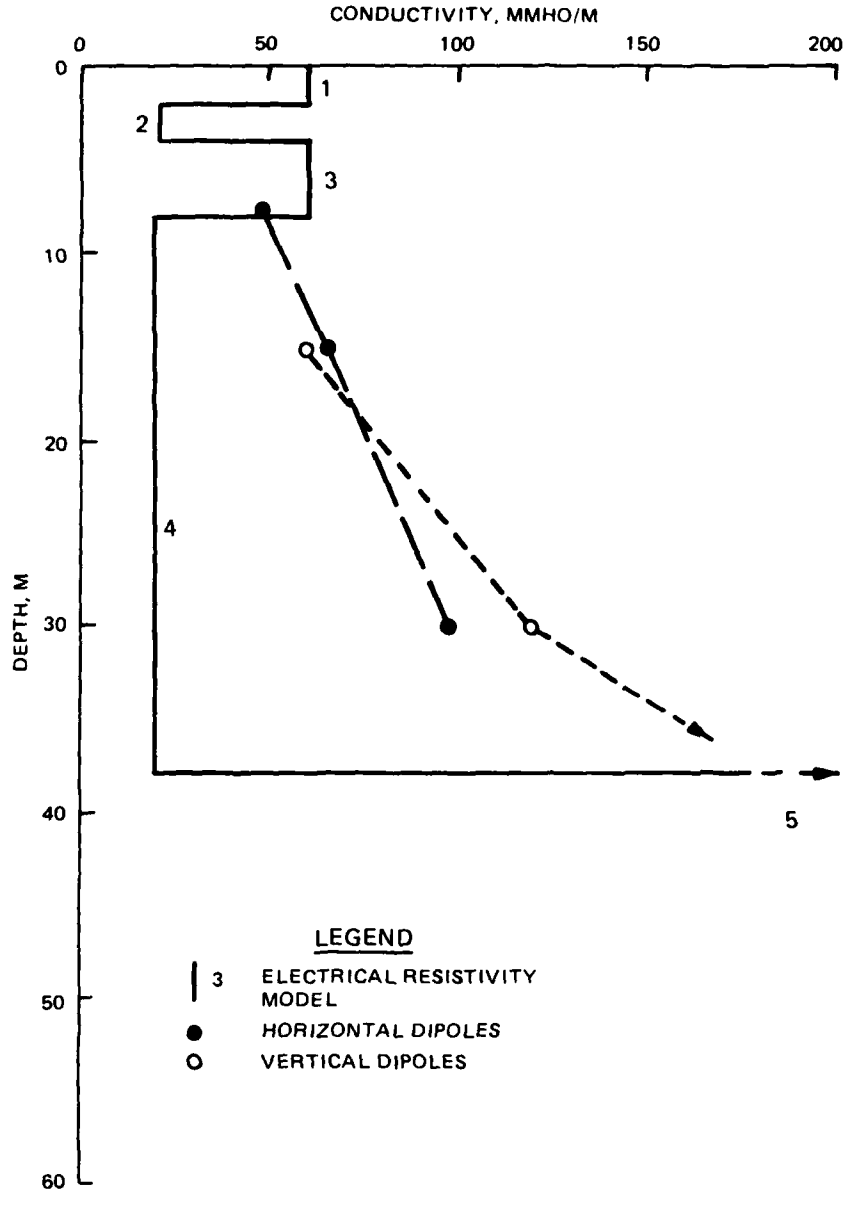

Figure 15. EM 34 data plotted at rules-of-thumb depths of investigation compared to electrical resistivity model for B-30

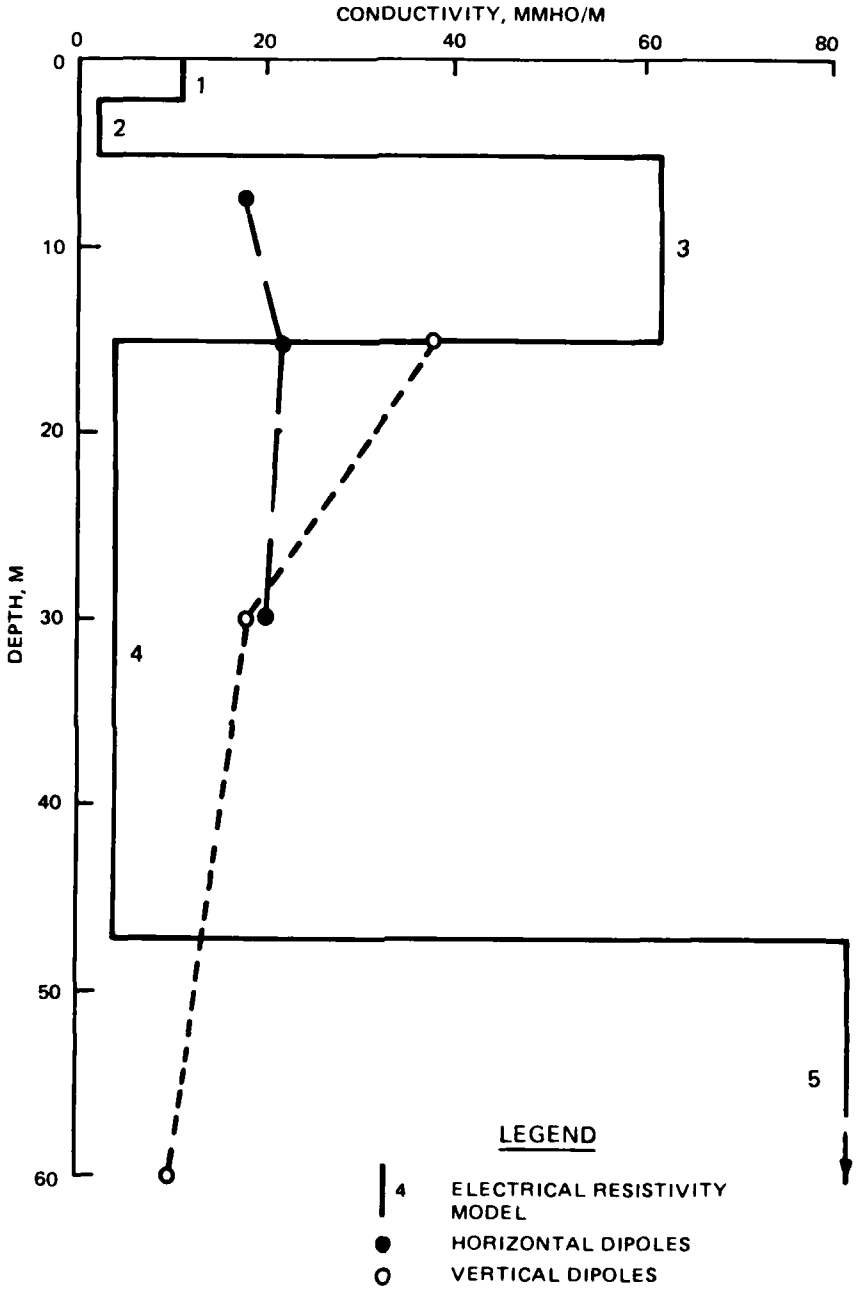

Figure 16. EM 34 data plotted at rules-of-thumb depths of investigation compared to electrical resistivity model for T-14

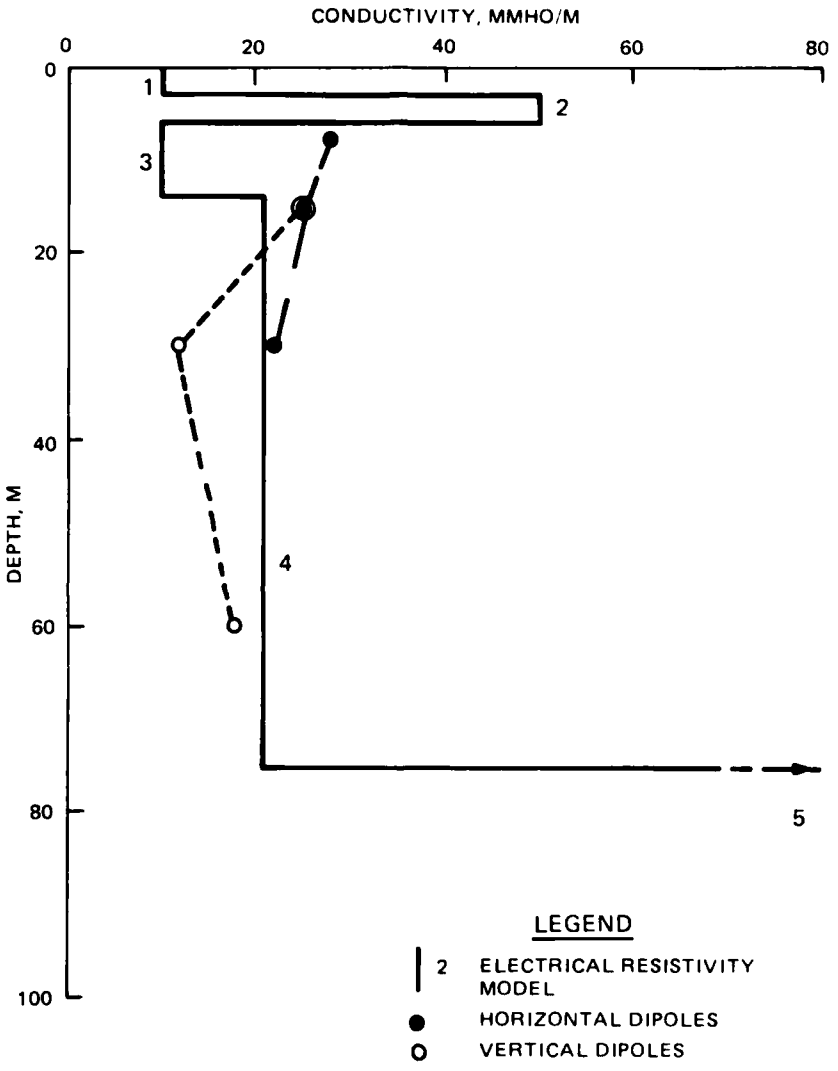

Figure 17. EM 34 data plotted at rules-of-thumb depths of investigation compared to electrical resistivity model for MAR

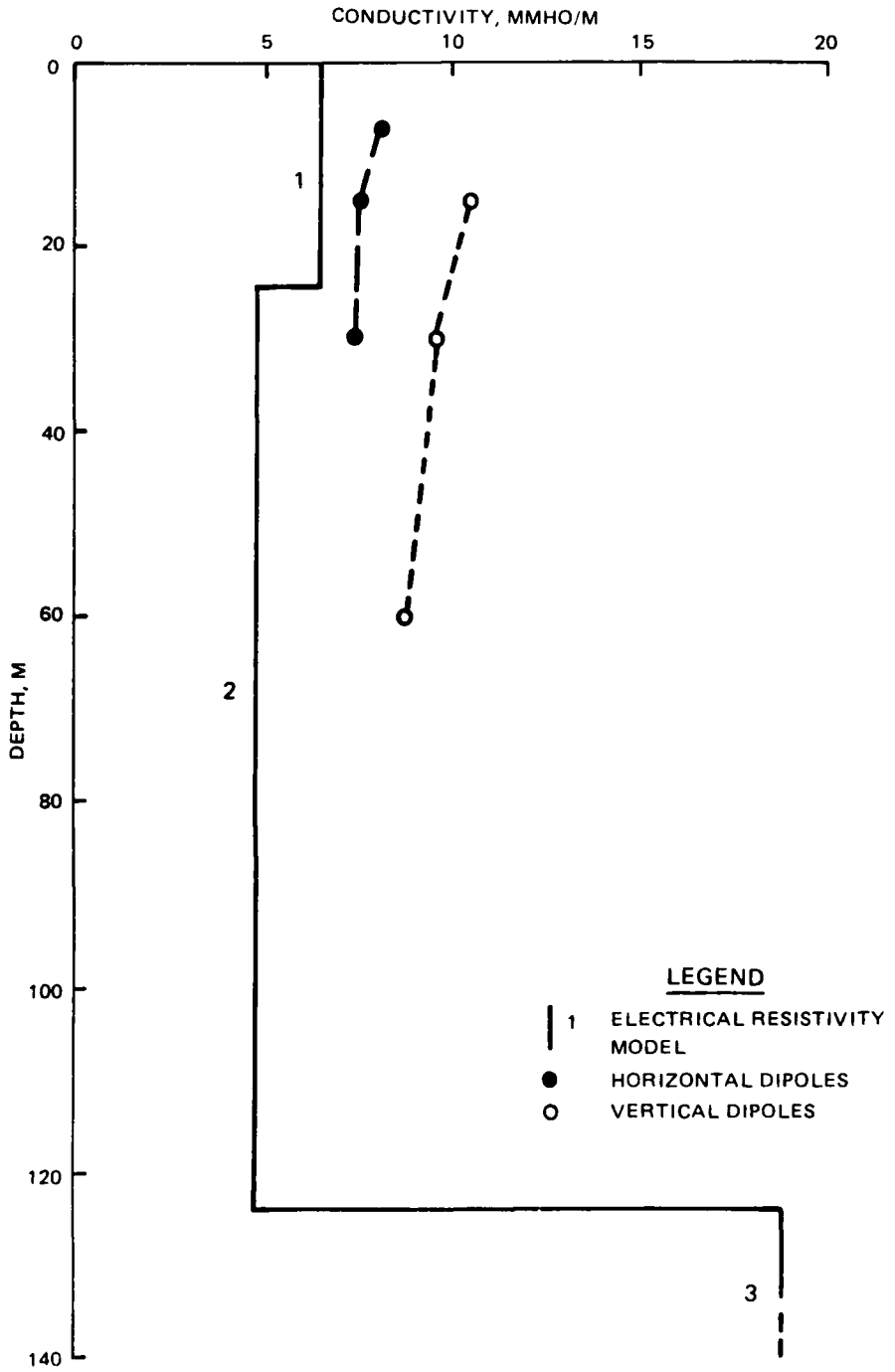

Figure 18. EM 34 data plotted at rules-of-thumb depths of investigation compared to electrical resistivity model for SW-19

used for profiling surveys, where the rules of thumb are used to assign an approximate depth of investigation for the profiles.

Two-layer response interpretations

53. Due to the small number of apparent conductivity values that can be obtained at a given location with the EM 34, interpretations of sounding data are limited to two layers. However, even when more than two layers are present at a given location, an equivalent two-layer model can be interpreted if the location exhibits a two-layer EM response. A two-layer EM response is characterized by:

a. The apparent conductivities for both the V and H dipole orientations will either monotonically increase or decrease.

b. If the two sets of apparent conductivities both increase, the V dipole data will consistently be larger in value than the H dipole data; or if both sets decrease, the V dipole data will consistently be smaller than the H dipole data.

c. The V and H dipole apparent conductivities will lie on sounding curves that can be calculated using the cumulative response functions.

54. McNeill (1980b) discusses two approaches for interpreting two-layer response curves: (a) curve matching, and (b) direct calculation using the apparent conductivity relation. Curve matching is accomplished by plotting the field data on log graph paper and adjusting the data points to lie on master curves plotted on log paper with the same modulus. The coordinate axes of the master curves are σ_A/σ_1 and z_1/R, where σ_1 and z_1 ($= z_{1b} = h_1$) are the conductivity and thickness of the first layer. The field data for $R = 40$ m are plotted at an arbitrary horizontal axis location, and the $R = 20$ m and $R = 10$ m data points are plotted at successive factors of two distances to the right of the $R = 40$ m location.

55. The apparent conductivity relation for two layers is

$$\sigma_A(R) = \sigma_1 \left[1 - R_z^{V,H}\left(\frac{z_1}{R}\right)\right] + \sigma_2 R_z^{V,H}\left(\frac{z_1}{R}\right) \qquad (24)$$

Evaluating Equation 24 for three apparent conductivity values measured with either the V or H dipole orientations yields three equations that can be solved for three unknowns z_1, σ_1, and σ_2.

56. An examination of the data in Table 5 reveals that only B-30 and SW-19 exhibit an apparent two-layer response. However, neither the B-30 nor the SW-19 data can be satisfactorily fit to the master curves of McNeill (1980b). In all cases except T-14, the H dipole data are sufficiently well

behaved (can be fit approximately to an H master curve) that calculation of an equivalent two-layer model using Equation 24 is possible. Table 6 gives the

Table 6

Two-Layer Equivalent Models

Location	Model Parameters
HTA-1*	z_1 = 15 m
	σ_1 = 8.8 mmho/m
	σ_2 = 5.3 mmho/m
B-30*	z_1 = 45 m
	σ_1 = 15 mmho/m
	σ_2 = 180 mmho/m
MAR*	z_1 = 3.2 m
	σ_1 = 28 mmho/m
	σ_2 = 18 mmho/m
SW-19**	z_1 = 13 m
	σ_1 = 12 mmho/m
	σ_1 = 8.8 mmho/m

* Model parameters calculated from H dipole data.

** Model parameters calculated from V dipole data.

calculated two-layer equivalent models. Comparison of the models in Table 6 with the electrical resistivity sounding models in Figures 14, 15, 17, and 18 indicates:

HTA-1 - The two-layer equivalent model successfully "averages" the upper three layers shown in Figure 14; z_1 is 17 percent shallower than the interface depth between layers 2 and 3 in Figure 14, and σ_1 and σ_2 appear to be "averages" of layers 1 and 2 and layers 2 and 3, respectively.

B-30 - The two-layer equivalent model successfully predicts the high-conductivity basement (layer 5 in Figure 15) although the interface is 18 percent deeper than the interface between layers 4 and 5 in Figure 15, and σ_1 and σ_2 are under-predicted compared to layers 1-4 and layer 5, respectively.

MAR - In the two-layer equivalent model, σ_1 effectively averages layers 1 and 2 and σ_2 averages layers 3 and 4, while the interface depth z_1 seems somewhat too shallow (Figure 17).

SW-19 - In the two-layer equivalent model, σ_1 and σ_2 overestimate the values shown in the model in Figure 18; also, the interface depth z_1 is nearly 50 percent shallower than the interface between layers 1 and 2.

Comparison of multilayer response calculations with field data

57. Apparent conductivities can be calculated for the layered models shown in Figure 14-18 using the response relations illustrated in Figure 9. Table 7 compares the measured apparent conductivities with those computed using the response relations. There is clearly little correlation between the measured and calculated apparent conductivities. For HTA-1, SW-19, and T-14, the data are comparable in magnitude, but the trends are not the same. For

Table 7

Comparison of Measured and Calculated Apparent Conductivities

Location	Coil Spacing m	Vertical Dipole Orientation, mmho/m		Horizontal Dipole Orientation, mmho/m	
		Measured	Calculated	Measured	Calculated
HTA-1	10	9.6	8.3	8.2	7.0
	20	8.4	7.3	7.7	7.4
	40	15	5.3	7.0	6.8
B-30*	10	60	420	48	235
	20	120	785	65	420
	40	Very large	1,410	98	765
T-14	10	95	35	45	24
	20	45	40	54	31
	40	23	44	50	37
MAR*	10	25	220	28	119
	20	11	414	25	218
	40	18	787	23	410
SW-19	10	10.5	6.7	8.1	6.6
	20	9.6	7.0	7.6	6.7
	40	8.8	7.6	7.5	7.0

* For B-30 and MAR, σ_5 = 3,000 mmho/m for the multilayer response calculations.

B-30, the data trends are the same, but the calculated magnitudes are much larger than the measured data. In the case of T-14, both the magnitudes and the trends differ significantly.

58. For all five cases, the multilayer response calculations predict apparent conductivities with magnitudes and trends which are controlled and usually dominated by the conductivity of the deepest layer. As already noted, however, with regard to Figures 14-18, the measured apparent conductivities show a response reflecting the intervening layers. The large calculated apparent conductivity values for B-30 and MAR suggest conditions under which the EM 34 should not be expected to work well (see Figure 7), although the measured values for these sites are consistent with models deduced from the resistivity soundings. These results suggest the multilayer response calculations should be used with caution for predicting EM-34 response, particularly when deeper layers in the model have much larger conductivity than the shallower layers.

Ground-water assessments

59. The anticipated or possible roles for CW EM methods in ground-water assessments were reviewed in Part III. The conclusions regarding the potential of the EM 34 (and similar devices with limited numbers of frequency and Tx-Rx spacing combinations) for ground-water assessments do not hold in general for CW EM systems. As a stand-alone method, the EM 34 gives only very limited clues to the ground-water potential at a given location. The apparent conductivity data for B-30, for example, indicate highly conductive conditions prevailing at depth ≥30 m, which could be a massive clay layer but is more likely saline water. Thus, potable water would be shallow at B-30; however, high conductivities evident even at 10-m loop spacing indicate fine-grained sediments, so water production from a well would likely be low.

60. For SW-19, the low conductivities indicate coarse-grained sediments or massive low-porosity rock. The geologic setting precludes the possibility of massive low-porosity rock at shallow depths. If coarse-grained sediments persist to considerable depth, a good aquifer is indicated, but the ground-water table must be >40 to 60 m deep. Based on the known hydrogeological conditions at B-30 and SW-19, the clues for the apparent conductivity data are good. For HTA-1 the apparent conductivity data could be misleading if the location of the nearby water pipe were not known, since the data could be interpreted as indicative of a good aquifer with a water table at a depth of

≤40 m. The T-14 and MAR apparent conductivity results are ambiguous.

Geological Model and EM Survey Results: Fort Carson, Colo.

Field procedures

61. A 700-m survey line was established at the Fort Carson site; soundings were conducted perpendicular to the survey line every 20 m along the line. Also, an EM sounding was conducted on an outcrop of Dakota Sandstone near the 700-m survey line at Fort Carson.

62. According to Leonard (1984), the dip of the Dakota Sandstone is very steep near its outcrop and decreases to the northeast. Thus, the use of an average regional dip for the Dakota Sandstone to produce the model in Figure 13 is incorrect. Site reconnaissance verified the extent and dip of the exposed Dakota Sandstone surface east of Turkey Creek. Leonard (1984) and the site reconnaissance were used to produce the revised geological model shown in Figure 19, where the top of the Dakota Sandstone is dashed to indicate the uncertainty between the outcrop and the known depth at the well.

63. The inferred top of the Dakota Sandstone is at evaluation 1,661 m beneath the location of WES-4 and is placed midway between seismic and electrical resistivity interfaces near the same elevations. Thus, the Dakota Sandstone is interpreted to have a seismic (p-wave) velocity of 3,200 m/sec and an electrical resistivity of 55 ohm-m; these geophysical parameter values are entirely consistent with those expected for a saturated sandstone.

64. Location of EM survey line is shown in Figure 12 and is approximately 300 m south of the cross-section line (Figure 19). The EM survey line crosses surficial soils consisting predominantly of silts and clays except at the dry creek bed approximately 200 m east of Turkey Creek, where there are poorly graded sands and silts (Dames and Moore, Inc. 1978). There is no exposure of the Dakota Sandstone beneath the EM survey line, and the sandstone is not visible in the low creek bluff at the western end of the line. Figure 20 shows the surface topography along the survey line and projects the top of the Dakota Sandstone from the cross section shown in Figure 19 assuming no dip to the south. The sands and silts along the dry creek bed are consistent with the position of the Dakota Sandstone. The surficial silts and clays adjacent to Turkey Creek may be an overbank veneer.

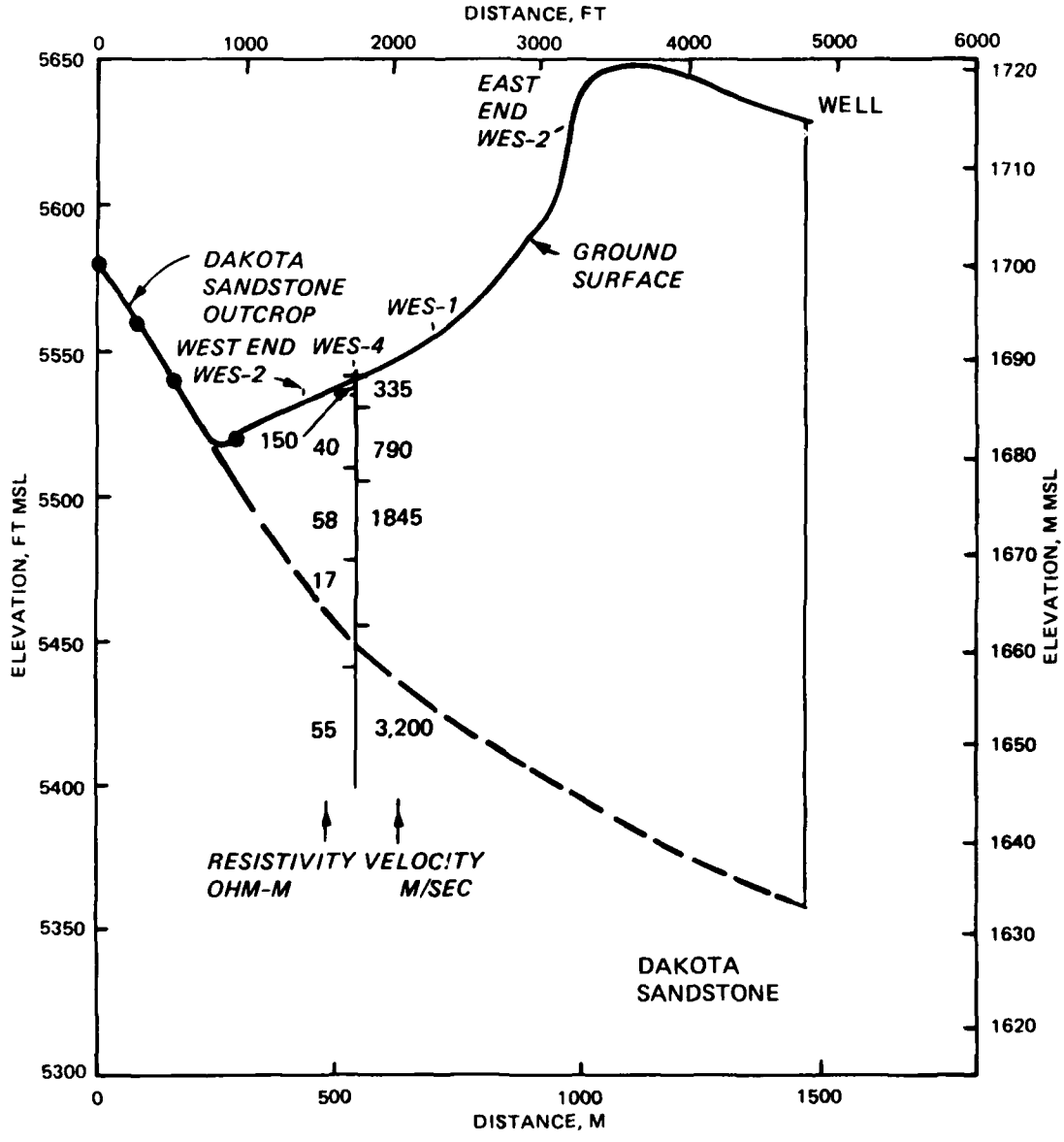

Figure 19. Revision of cross section in Figure 13 to include increasing dip of Dakota Sandstone to match dip of the outcrop, Fort Carson

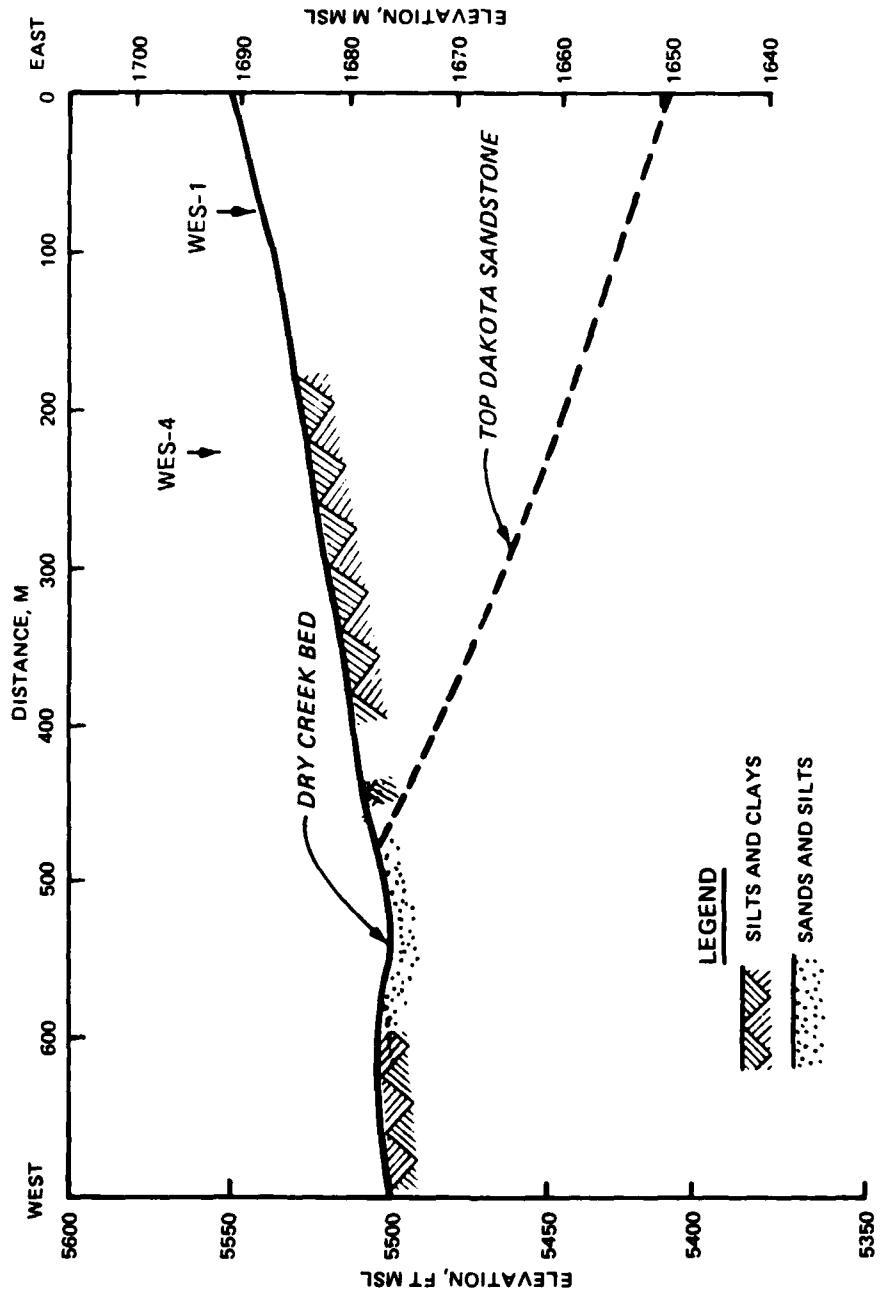

Figure 20. Cross section beneath the EM survey line, Fort Carson

EM survey results

65. Results of the EM survey at Fort Carson are shown in Figure 21 as 10-, 20-, and 40-m Tx-Rx spacing profiles; each profile shown includes both V and H dipole orientation results. Also, the results of the sounding on the sandstone outcrop north of the survey line are shown as data points on the conductivity axis. all of the profiles have qualitatively the same trends: (a) high conductivities, ~30 to 50 mmho/m, from 0- to 300-m profiles position; (b) decrease to a lower conductivity, ~10 to 20 mmho/m, over the range 300 to 500 m; and (c) increase to an intermediate conductivity, ~20 to 30 m, over the range 500 to 700 m. The data are somewhat erratic, particularly for the eastern part of the survey line. The average apparent conductivity values for entire profile lines increase as Tx-Rx spacing increases; this indicates a general increase in conductivity with depth at the site. All of the data shown in Figure 21 were acquired in about 3 hr.

66. The EM sounding results on the sandstone outcrop display a monotonic increase in apparent conductivity with increasing Tx-Rx spacing and, hence, depth. These results are consistent with a model for the sandstone which is dry at the surface, becomes moist below the surface, and finally becomes saturated. The interpreted resistivity for the saturated sandstone of 55 ohm/m (see paragraph 63) corresponds to a conductivity of 18 mmho/m, which agrees with the EM sounding results. Also, in the 400- to 500-m profile range, all results approach the corresponding apparent conductivity values measured at the same Tx-Rx spacing on the sandstone outcrop, in agreement with the model shown in Figure 20.

67. The features and trends of the EM profiles in Figure 21 can be explained in terms of the model in Figure 20. The conductivity highs in Figure 21 at profile positions 80 and 100 m, particularly in the H profile data, are associated with Lytle Road (see Figure 12), as both positions are in small ravines adjacent to the road. The high conductivities on the eastern half of the profile line are due to the surficial silts and clays and underlying shale and bentonite (see well log in Figure 13). The apparent conductivity increases for $R = 20$ m compared to $R = 10$ m are due to including more higher conductivity shale within the depth of investigation. For $R = 40$ m, the low-conductivity Dakota Sandstone begins to influence the apparent conductivities, particularly for the V dipole orientation, on the eastern half of the profile line. For all three coil spacings, the data

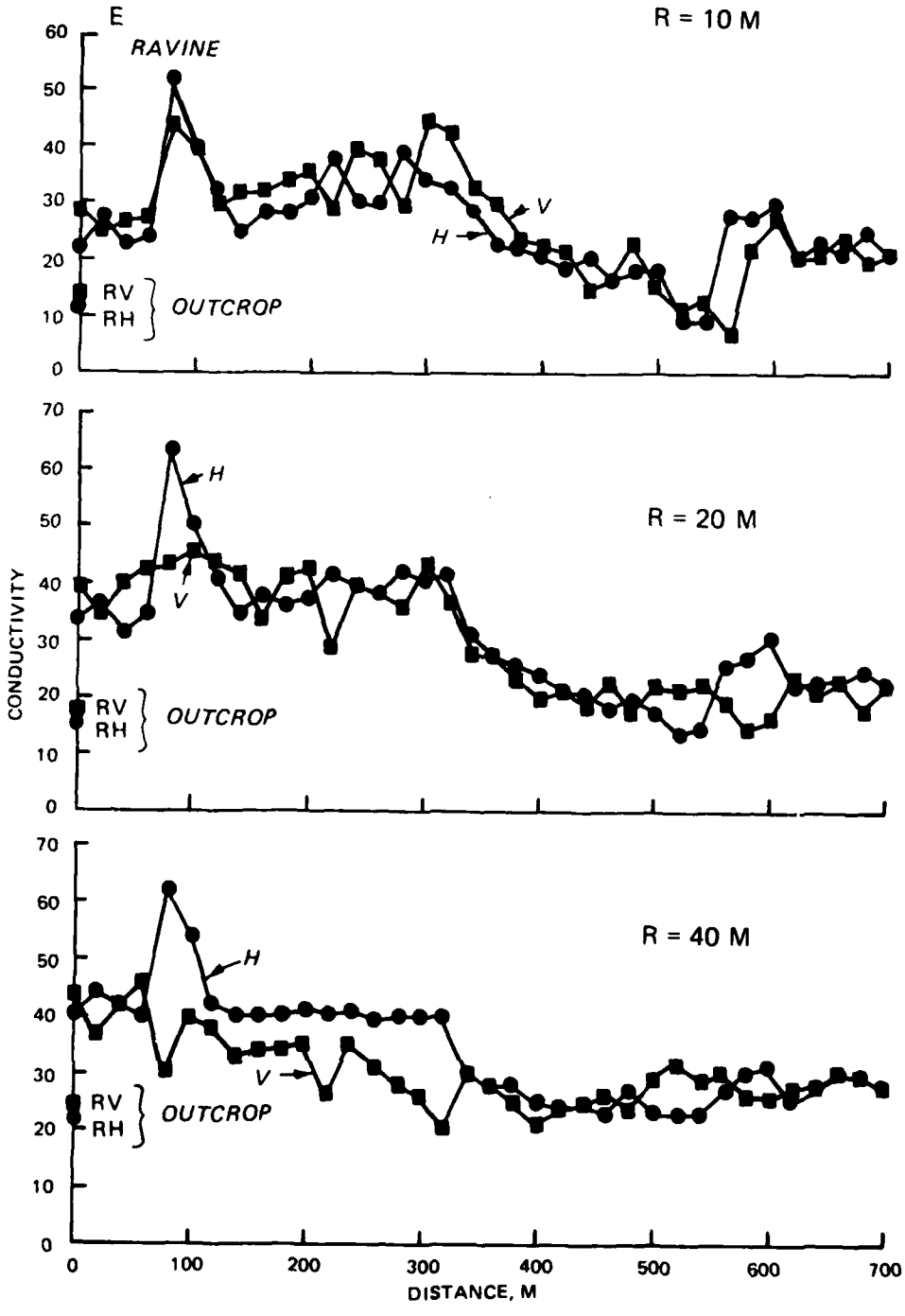

Figure 21. EM 34 survey results, Fort Carson

indicate the decreasing depth to the Dakota Sandstone from east to west along the line by a decrease in conductivity: the decrease begins at 360 m for R = 10 m ; the decrease begins at 320 m for R = 20 m ; the decrease begins at 240 m for R = 40 m for the V case. Finally, the small increase in conductivity on the western end of the line is apparently due to the overbank veneer of silts and clays. These results indicate considerable possibilities for stratigraphic mapping, but only if geologic control ("ground truth") is available.

PART V: SUMMARY, CONCLUSIONS, AND RECOMMENDATIONS

Summary

68. This report reviews the concept of a particular type of electromagnetic (EM) geophysical method applied to ground-water exploration and assessment. The method utilizes a small loop transmitter, which is excited with a continuous wave EM signal. The magnetic field generated by the transmitter couples inductively with subsurface geological materials and generates eddy currents. The secondary magnetic fields generated by the eddy currents couple inductively with a small loop receiver. The specific system type considered in this report operates under conditions which allow a "small induction number approximation" to be made. This approximation allows the receiver response to be calibrated directly in terms of apparent ground conductivity. By operating the system at multiple transmitter and receiver coil spacings and multiple transmitter frequencies, it is possible to conduct EM soundings.

69. A specific CW EM system was field tested at White Sands, N. Mex., and Fort Carson, Colo., at locations where previous geophysical surveys were conducted using seismic and electrical resistivity methods. For the White Sands EM surveys, a critical evaluation of data interpretation procedures is presented. Specifically, the EM interpretations are compared to models deduced from the previous geophysical work at the locations. At Fort Carson, an EM sounding was conducted at 20-m intervals along a 700-m profile line. Also, an EM sounding was conducted on an outcrop of Dakota Sandstone.

Conclusions

70. The results of an EM sounding can be interpreted, in principle, to yield a model of the vertical variation in electrical conductivity in the subsurface. In some cases the conductivity model can be interpreted in terms of a hydrogeological model, although supplementary geological data or complementary geophysical data are usually required. Analysis of the White Sands EM survey results indicates that multilayer response calculations, for predicting the low induction number performance of the device, should be used with caution because the response functions overpredict the proportion of the response from deeper layers. For three of the five cases, two-layer equivalent model

interpretations of the EM data are useful and correlate satisfactorily with resistivity models. The most useful interpretation procedure is to assign measured apparent conductivities of rule-of-thumb depths of investigation and use the model only as a qualitative indicator of the conductivity versus depth variation. At Fort Carson, the conductivities measured on the outcrop agreed with values deduced for the sandstone in the subsurface from a resistivity sounding. The EM data along the Fort Carson profile line agreed well with a geological model for the site deduced from available geologic information, site reconnaissance, and previous geophysical surveys.

71. The EM device evaluated in this study is lightweight and easy to operate in the field; surveys proceed rapidly. These comments apply in general to CW EM systems. The device considered in this report could not stand alone nor replace electrical resistivity in a complementary methods approach for ground-water detection and assessment. However, the device can be useful as a rapid survey technique to supplement resistivity surveys in a complementary methods approach. The CW EM methods are not limited to the small number of conductivity determinations (coil spacing-frequency combinations) of the device considered here. Currently available CW EM systems with greater capability and applicability, however, are larger and more cumbersome to use, and the data interpretation is not as straightforward.

Recommendations

72. The next generation of devices, similar in size and simplicity of operation to the device evaluated in this study, is expected to have greater versatility. For example, an EM device with three transmitter frequencies, three Tx-Rx spacings, and two coil orientations could yield 18 EM field component measurements. Conversion of the measurements to apparent conductivity or resistivity values using a hand-held calculator or microcomputer would yield a well-defined sounding curve. The advantages of obtaining a sounding curve amenable to a multilayer interpretation are greater than the advantage of having a device calibrated to yield apparent conductivity directly by satisfying a low induction number criterion. Full advantage should be taken of microprocessor technology in the design of the new devices to automate both data acquisition and sequencing and data storage.

REFERENCES

Butler, Dwain K., and Llopis, Jose L. 1984. "Military Hydrology; Report 6: Assessment of Two Currently 'Fieldable' Geophysical Methods for Military Ground-Water Detection," Miscellaneous Paper EL-79-6, US Army Engineer Waterways Experiment Station, Vicksburg, Miss.

Cruz, R. R. 1981. "Annual Water-Resources Review, White Sands Missile Range, New Mexico," Open File Report 82-757, US Geological Survey, Albuquerque, N. Mex.

Dames and Moore, Inc. 1978. "Fort Carson, Colorado, Terrain Analysis," Contract No. DACA87-77-C-0059, prepared for US Army Engineer Topographic Laboratory, Fort Belvoir, Va.

Dardeau, E. A., and Zappi, M. A. 1977. "Environmental Baseline Descriptions for Use in Management of Fort Carson Natural Resources; Report 5: General Geology and Seismicity," Technical Report M-77-4, US Army Engineer Waterways Experiment Station, Vicksburg, Miss.

Electromagnetic Surveys, Inc. (EMSI). 1979. "An Evaluation of Horizontal Loop Electromagnetic Sounding in Exploration for Ground Water in the Central Valley of California," Report No. 7902, Berkeley, Calif.

Grant, F. S., and West, G. F. 1965. Interpretation Theory in Applied Geophysics, McGraw-Hill Book Company, New York.

Greenhouse, J. D., and Slaine, D. S. 1983. "Predictive Modeling and Surface Mapping of Contaminated Groundwater Plumes with Electromagnetic Resistivity Techniques," Proceedings of Fifty-Third Annual International Meeting, Society of Exploration Geophysicists, Las Vegas, Nev., pp 90-93.

Kaufman, Alexander A., and Keller, George V. 1983. Frequency and Transient Soundings, Elsevier Science Publishing Company, New York.

Keller, George V., and Frischknecht, Frank C. 1966. Electrical Methods in Geophysical Prospecting, Pergamon Press, New York.

Leonard, G. J. 1984. "Assessment of Water Resources at Fort Carson Military Reservation near Colorado Springs, Colorado," Water Resources Investigation Report 83-4270, US Geological Survey, Lakewood, Colo.

McNeill, J. D. 1980a. "Electromagnetic Terrain Conductivity Measurement at Low Induction Numbers," Technical Note TN-6, Geonics Limited, Ontario, Canada.

_____. 1980b. "EM 34-3 Survey Interpretation Techniques," Technical Note TN-8, Geonics Limited, Ontario, Canada.

_____. 1982. "Electromagnetic Resistivity Mapping of Contaminant Plumes in Management of Uncontrolled Hazardous Waste Sites," Hazardous Material Control Research Institute, Silver Springs, Md., pp 1-6.

Palacky, G. J., Ritsema, I. L., and De Jong, S. J. 1981. "Electromagnetic Prospecting for Groundwater in Precambrian Terrains in the Republic of Upper Volta," Geophysical Prospecting, Vol 29, pp 932-955.

Patra, H. P., and Mallick, K. 1980. Geosounding Principles; Vol 2: Time-Varying Geoelectric Soundings, Elsevier Science Publishing Company, New York.

Ryu, Jisoo, Morrison, H. Frank, and Ward, Stanley H. 1972. "Electromagnetic Depth Sounding Experiment Across Santa Clara Valley," Geophysics, Vol 37, No. 2, pp 351-374.

Stewart, Mark T. 1981. "Evaluation of Electromagnetic Terrain Conductivity Measurements for Detection and Mapping of Salt Water Interfaces in Coastal Aquifers," Project Report, Grant No. A-043-FLA, University of South Florida, Tampa, Fla.

_____. 1982. "Evaluation of Electromagnetic Terrain Conductivity Methods for Rapid Detection of Salt Water Interfaces in Coastal Aquifers," Ground Water, Vol 20, No. 5.

Sweeney, Jerry J. 1984. "Comparison of Electrical Resistivity Methods for Investigation of Ground Water Conditions at a Landfill Site," Ground Water Monitoring Review, Vol 4, No. 1, pp 52-59.

Wait, James R. 1982. Geo-Electromagnetism, Academic Press, New York.

END

10-86

DTIC